

Examination of the role of dreissenids and macrophytes in the phosphorus dynamics of Lake Simcoe, Ontario, Canada



Alexey Gudimov^a, Dong-Kyun Kim^a, Joelle D. Young^b, Michelle E. Palmer^b, Maria Dittrich^a, Jennifer G. Winter^b, Eleanor Stainsby^b, George B. Arhonditsis^{a,*}

^a Department of Physical & Environmental Sciences, University of Toronto, Toronto, Ontario M1C 1A4, Canada

^b Environmental Monitoring and Reporting Branch, Ontario Ministry of the Environment, Toronto, Ontario M9P 3V6, Canada

ARTICLE INFO

Article history:

Received 28 June 2014

Received in revised form 22 November 2014

Accepted 25 November 2014

Available online 3 December 2014

Keywords:

Eutrophication

Macrophytes

Dreissenids

Nutrient recycling

Sediment diagenesis

Phosphorus dynamics

ABSTRACT

Our study examines the relative importance of the causal linkages between exogenous total phosphorus (TP) loading and internal nutrient recycling with the water quality conditions in Lake Simcoe, Ontario, Canada. We enhance the mechanistic foundation of a simple TP mass-balance model, originally developed to guide the eutrophication management in the system. The structural improvements include the incorporation of macrophyte dynamics, the explicit representation of the role of dreissenids in the system, and the improved portrayal of the interplay between water column and sediments. Our model provides good agreement with the observed TP variability in the system during the study period (1999–2007). Consistent with empirical evidence, our model predicts that macrophyte uptake from the interstitial waters is responsible for a significant loss of P from the sediments. Our model also suggests that dreissenids filter a considerable amount of particulate P from the water column, but the effective clearance rate is significantly lower with a substantial amount of the filtered particles (>85%) returned into the water column as faeces, pseudofaeces or other metabolic excreta. P diffusive fluxes from the sediments account for about 30–35% of the exogenous P loading in Lake Simcoe. The sediments in the main basin are mostly driven by fast diagenetic processes of settling organic matter from the epilimnion, suggesting an internal P loading of 9.2 tonnes yr⁻¹. Finally, our study attempts to explain the lack of distinct decreasing trends in ice-free TP concentrations after the invasion of dreissenid mussels, suggesting that the presence of active nutrient recycling pathways, potentially magnified by the particular morphological features and hydrodynamic patterns of Lake Simcoe, could counterbalance the direct effects of dreissenid filtration.

© 2014 Elsevier B.V. All rights reserved.

1. Introduction

The invasion of dreissenid mussels has been responsible for a major restructuring of the biophysical environment in many parts of the Laurentian Great Lakes, with profound alterations on the nutrient dynamics in the littoral zone (Coleman and Williams, 2002). The near-shore shunt (sensu Hecky et al., 2004) has been hypothesized to impact the fate and transport of particulate matter, and subsequently alter the relative productivity of inshore sites and their interactions with the offshore areas. Most notably, dreissenid mussels may filter twice as many food particles as they can ingest, and therefore a large portion of the filtered food items is excreted in soluble form or released as (pseudo)faeces (Vanderploeg et al., 2001). When we also consider that the particulate matter is subject to bacterial mineralization, it can be inferred that dreissenids are likely to mediate nutrient cycling and may significantly modulate the nearshore nutrient concentrations

(Bierman et al., 2005). In regard to the littoral algal assemblage, the establishment of dreissenid mussels has been associated with both desirable (e.g., phytoplankton biomass decline, gradual disappearance of *Aphanizomenon* and *Oscillatoria*) and undesirable (e.g., *Microcystis* increase) changes in the overall ecosystem integrity (Nicholls et al., 2002; Vanderploeg et al., 2001). The structural changes in the phytoplankton community composition could stem directly from the feeding selectivity of dreissenids or indirectly from the improvements in the transparency of the water column, but the role of the feedback loop associated with their nutrient recycling activity may be another important factor (Bierman et al., 2005).

In Lake Simcoe, the initial year with discernible dreissenid production was 1994, while abundant colonies of juvenile and adult mussels first occurred on rocky substrates throughout the spring and summer growing season in 1996 (Evans et al., 2011). In the main basin of Lake Simcoe, dreissenid mussel distribution is determined by a complex interplay among lake depth, substrate availability and exposure to wave disturbance (Ozersky et al., 2011). Specifically, the highest dreissenid biomass is typically found at areas of intermediate

* Corresponding author. Tel.: +1 416 208 4858; fax: +1 416 287 7279.
E-mail address: georgea@utsc.utoronto.ca (G.B. Arhonditsis).

depth, where water movement is high enough to ensure that the lake bottom is dominated by rocky substrates but not excessively high to cause catastrophic disturbances to the dreissenid community. On the other hand, Ozersky et al. (2011) were not able to identify a clear causal connection between hydrodynamic regime and dreissenids in Cook's Bay, a shallow bay at the south end of the lake where macrophyte growth is abundant. They concluded that the nature of the macrophyte assemblage (composition, taxon-specific abundance) may be the predominant factor in shaping the dreissenid mussel distribution in this embayment. Schwalb et al. (2013) reported a counterintuitive positive relationship between phytoplankton abundance and dreissenid biomass in the nearshore, which was attributed to the horizontal advection and/or the internal wave-mediated transport of deep chlorophyll *a* maxima that can temporarily counteract the algal depletion by mussels. Moreover, the dreissenid-colonized sediments were found to act as a net source of dissolved nutrients to the water column due to their considerably high excretion rates of dissolved phosphorus and ammonia (Ozersky et al., 2013). Not surprisingly, the same sites were characterized by higher amounts of periphyton biomass, primary production, and community respiration relative to sites where mussels were fairly low.

An important implication of the causal linkage between dreissenids and nutrient variability in the littoral zone is the weakening of the external loading signal, which led Hecky et al. (2004) to question whether conventional TP mass-balance models developed during the pre-dreissenid period in the Great Lakes were structurally adequate during the post-dreissenid era. In this regard, Zhang et al. (2013) showed in the upper Bay of Quinte that failure to explicitly account for the role of dreissenids (or other factors associated with the internal nutrient loading) compromised the capacity of a model to capture the TP peaks typically experienced towards the late summer–early fall period. In particular, the modelled range of the monthly TP concentrations was much narrower than the actual values and the predicted patterns failed to reproduce the substantial inter-annual variability characterizing the system (Zhang et al., 2013). In Lake Simcoe, Gudimov et al. (2012) recently introduced a spatially-explicit simple mass-balance model forced with idealized sinusoidal loading to predict total P concentrations. The study reported two-fold discrepancy between empirical gross and predicted net TP sedimentation rates, presumably reflecting the role of macrophytes and dreissenids, the sediment resuspension induced by wind forcing, the diffusive release of P from the sediments, and the complex interplay between offshore waters and the two embayments of Lake Simcoe (Cook's Bay and Kempenfelt Bay). In this regard, Nürnberg et al. (2013) provided evidence of substantial internal loading in all lake sections, but especially in the stratified Kempenfelt Bay and the main basin. The same study also asserted that internal loading may also occur in the polymictic Cook's Bay, as the warmer temperatures may elevate the sediment oxygen demand and P release rates. By contrast, Dittrich et al. (2013) reported empirical estimates that were significantly lower than Nürnberg et al. (2013) internal loading fluxes (see also Discussion section).

In this study, we use mathematical modelling to test the hypothesis that the spatial and temporal variability of P in Lake Simcoe was predominantly driven by internal mechanisms following the establishment of dreissenids and the proliferation of macrophytes. First, we present the mechanistic foundation of phosphorus mass-balance model, recently developed by Kim et al. (2013), aiming to account for the role of macrophyte dynamics, to explicitly represent the impact of dreissenids in the system, and to sensibly portray the interplay between water column and sediments. We provide the rationale behind the model structure adopted, the simplifications included, and the mathematical formulations used. We show the results of a calibration exercise and examine the capacity of the model to sufficiently reproduce the observed patterns in Lake Simcoe during the 1999–2007 study period. We then present the findings of a local sensitivity analysis striving to

identify the most influential components of the model, and to shed light on the spatiotemporal role of the various ecological processes and cause–effect relationships as postulated by the model parameter specification. We also critically discuss several of the lessons learned from our modelling analysis regarding the ecosystem functioning relative to our contemporary understanding of the Lake Simcoe dynamics.

2. Methods

2.1. Site description-dataset

Lake Simcoe experienced severe eutrophication problems as a result of the agricultural activities and increasing urbanization in its catchment beginning in the 1930s (North, 2013). From 2004 to 2007, Lake Simcoe received P loads from fourteen municipal wastewater treatment plants (6 ± 1 tonnes yr^{-1}), atmospheric deposition (18 ± 4 tonnes yr^{-1}) and other non-point pathways, including runoff from agricultural, urban and natural areas (43 ± 5 tonnes yr^{-1}), and rural septic systems (4.4 ± 0.1 tonnes yr^{-1}) (LSRCA and MOE, 2012). The exogenous P loading determines the ambient lake total P levels and stimulates phytoplankton production, and the subsequent decomposition of the excessive organic matter in the sediments likely contributes to hypolimnetic dissolved oxygen (DO) depletion (Dittrich et al., 2013; McCulloch et al., 2013; Nicholls, 1997). Prior to the mid-1990s, end-of-summer hypolimnetic DO levels reached nearly lethal levels (<3 mg L^{-1}) for many coldwater fish species (Evans, 2007). As a result, fish abundance declined for several commercially important fish species, such as lake trout (*Salvelinus namaycush*), lake whitefish (*Coregonus clupeaformis*) and lake herring (*Coregonus artedii*) (Evans, 2007). To assist with the restoration of a self-sustaining coldwater fishery, the on-going reduction of point and non-point P inputs aims to control excessive phytoplankton biomass production and improve the end-of-summer volume-weighted hypolimnetic dissolved oxygen with a target minimum of 7 mg L^{-1} (Young et al., 2011).

Lake Simcoe is a well studied system with detailed long-term records of major sources and sinks of P at both lake top (water surface) and bottom (sediment bed) boundaries. The Ontario Ministry of the Environment (MOE) and Lake Simcoe Region Conservation Authority (LSRCA) have collected bi-monthly water temperature, water clarity and water quality samples from the ice-free period at different monitoring stations. Data on monthly tributary discharges and P exogenous loading into Lake Simcoe for the 1999–2007 period were provided by LSRCA and MOE (2006, 2012), based on the midpoint method of interpolation to fill the gaps between bi-monthly samples of TP concentrations and flow discharges. Wind data have been compiled from Weather Canada database in an hourly scale. Information on macrophyte abundance has been compiled from several published sources (Depew et al., 2011a,b; Ginn, 2011; LSRCA, 2011; Stantec, 2007), while dreissenids spatial distribution and physiological parameters have been studied by Ozersky et al. (2011, 2013) and Evans et al. (2011). Sediment profile measurements have been published in Dittrich et al. (2013) and include sediment porosity (ϕ), total phosphorus (TP_{sed}), organic bound P (OP_{sed}), particulate inorganic (PIP_{sed}), and dissolved inorganic (DIP_{sed}) P concentrations. Scenario analyses of sediment internal P loading reflect estimated fluxes presented in Dittrich et al. (2013) and Nürnberg et al. (2013). Organic microbial decomposition rates in sediments are based on the McCulloch et al. (2013) modelling study, while sediment burial rates at different monitoring stations have been adopted from Hiriart-Baer et al. (2011).

2.2. Model description

The present study is based on a TP mass-balance model that represents Lake Simcoe as four completely mixed tank reactors, while explicitly accommodating the stratification patterns typically shaping

the water quality patterns in Kempenfelt Bay, Cook's Bay and the main basin (Fig. 1). According to our model, the Lake Simcoe segmentation resembles Nicholls' (1997) conceptualization, in that the two embayments (Kempenfelt Bay and Cook's Bay) along with the shallow littoral zone at the East End (East Basin) are separated from the main basin (Fig. 1). The four epilimnetic segments are interconnected through bi-directional hydraulic exchanges to account for wind-driven flows and tributary discharges from adjacent watersheds. The present model follows the approach presented by Kim et al. (2013) to improve the fidelity of epilimnetic TP simulations through detailed specification of internal P recycling pathways (Fig. 2), such as the macrophyte dynamics and dreissenid activity as well as the fate and transport of P in the sediments, including the sediment resuspension, sorption/desorption in the sediment particles, and organic matter decomposition (see Table 1). Thus, the ordinary differential equations describing the dynamics of P in the water column consider all the external inputs, advective horizontal mass exchanges between adjacent segments, macrophyte uptake, macrophyte P release through respiration, dreissenid filtration, dreissenid excretion and pseudofeces egestion, vertical diffusive exchanges when stratification is established, and refluxes from the bottom sediments. The model considers a weighted average TP sedimentation rate to account for the differences in settling velocities of autochthonous and allochthonous biogenic particles (Ramin et al., 2011). Because the model does not distinguish between soluble and particulate P in the water column, the phytoplankton and detritus concentrations are introduced as forcing functions, which ultimately allow the characterization of the site-specific settling fluxes and the reproduction of the TP gradient from the eutrophic Cook's Bay to the mesotrophic main basin.

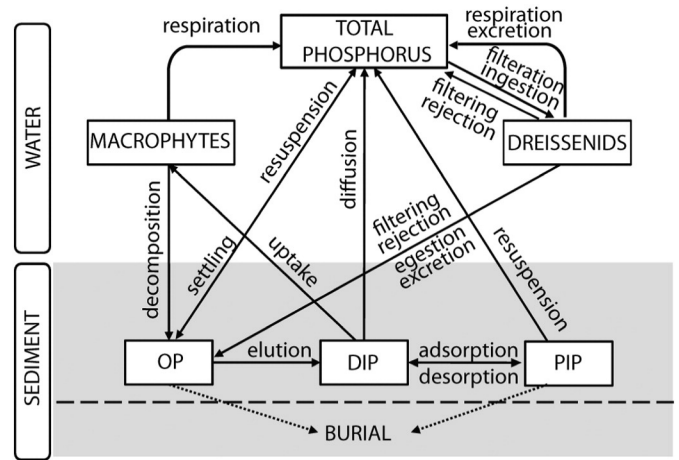


Fig. 2. Conceptual diagram of phosphorus pathways in P mass-balance model of Lake Simcoe.

2.2.1. Intersegment circulation flows

In the Gudimov et al.'s (2012) feedforward model, the hydraulic exchanges between the two embayments and the main basin have been reproduced through a set of annually averaged unidirectional net flows, which were subject to Bayesian updating. Here, we improve the representation of the horizontal advection patterns with the consideration of daily bi-directional flows while maintaining lake-wide hydraulic mass-balance. The embayment outflows comprise the watershed inflow discharges and the horizontal advection movement due to

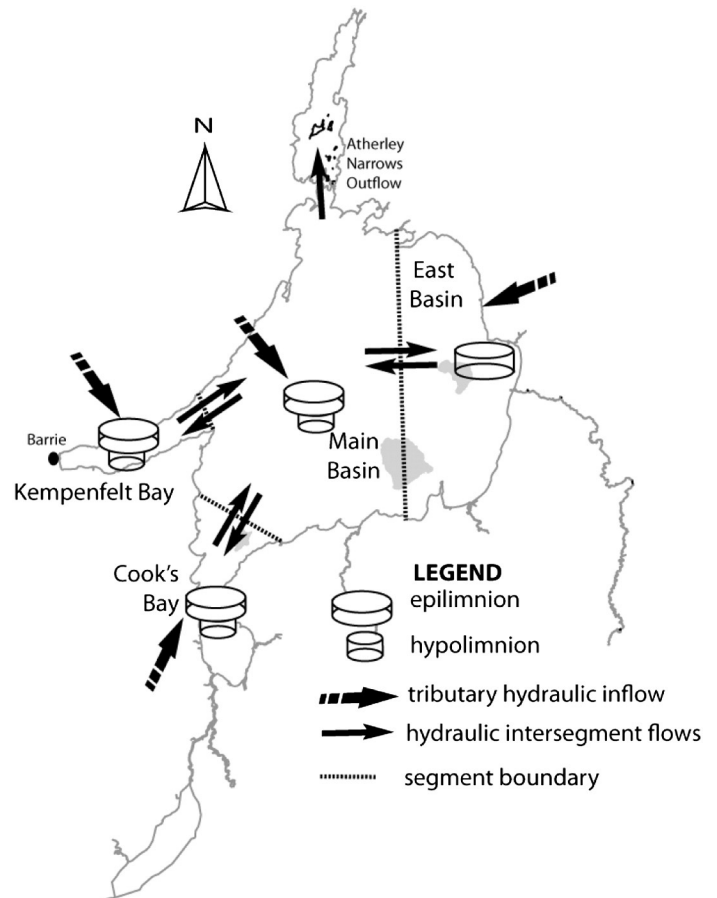
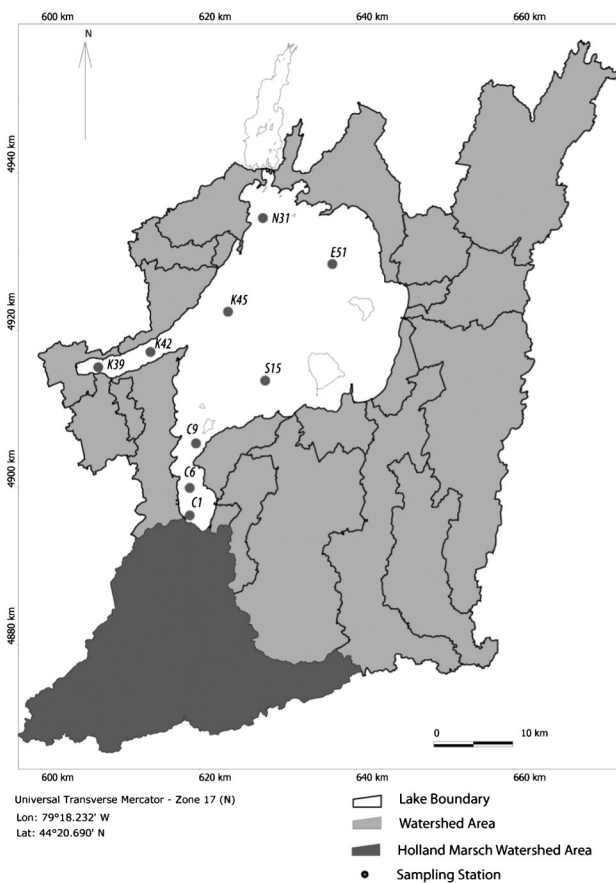


Fig. 1. Lake Simcoe map with adjacent watershed areas (left panel); Lake Simcoe spatial segmentation and intersegment flow diagram (right panel).

Table 1

Mathematical equations of the total phosphorus model.

Process	Symbol	Equation	
Water column	$\frac{dTP_w}{dt}$	$TP_{in} + TP_{sdR} + TP_{sdD} + TP_{macR} + TP_{zmR} + TP_{zmX} + TP_{zmRjw} - TP_{ws} - TP_{zmf} + [TP_{backflow} - TP_{out} + TPD_{Le, Lh}]$	
	TP_{sdR}	$\frac{A}{V_w} R_{resus}$	
	TP_{sdD}	$D_{sed}(DIP_{sed} - DIP_w)$	
	TP_{macR}	$\alpha_{mac} \frac{A}{V_w} (R_{mac} BP_{mac}) B_{mac}$	
	TP_{zmR}	$\frac{N_{ac} A}{V_w} BP_{zm} w_f R_{zm} B_{zm}$	
	TP_{zmX}	$\alpha_{zm} \frac{N_{ac} A}{V_w} BP_{zm} (1 - f_{OP-ZM}) w_f U_{zm} B_{zm}$	
	TP_{zmf}	$\frac{FT_{zm}}{V_w}$	
	TP_{zmRjw}	$(1 - \alpha_{sed})(FT_{zm} - w_f I_{zm} N_{ab} AB_{zm} BP_{zm})$	
	TP_{ws}	$\frac{V_s}{Z} \cdot TP_w$	
	V_s	$\frac{chla}{TP_w} \frac{PC}{chlaC} V_{s-chla} + (1 - \frac{chla}{TP_w} \frac{PC}{chlaC}) V_{s-pp}$	
	$TP_{backflow}$	$TP_w(\text{Main Basin}) \frac{Q_{backflow}}{V_w}$	
	TP_{out}	$TP_w(\text{Inshore Segment}) \frac{Q_{outflow}}{V_w}$	
	$TPD_{Le, Lh}$	$\frac{1}{V_{Le, Lh}(t)} \left[A_{Lh} \left\{ \frac{K_{str}/nstr(\Delta TP_{Le, Lh})}{\Delta z} \right\} \right]$	
	Macrophytes	$\frac{dB_{mac}}{dt}$	$(G_{mac} - R_{mac} - D_{mac}) \cdot B_{mac}$
		G_{mac}	$P_m \frac{DIP_{sed}}{K_p + DIP_{sed}} f_L(t)$
$f_L(t)$		$\frac{2.718 \cdot FD}{K_{ext} \cdot Z_{mac}} \{ e^{-x1} - e^{-x2} \}$	
$x1$		$\frac{I_0 e^{-K_{ext} Z_{mac}}}{FD \cdot I_{opt}}$	
$x2$		$\frac{I_0}{FD \cdot I_{opt}}$	
K_{ext}		$\alpha_1 + \alpha_2 chla$	
R_{mac}		$R_{mac20} \cdot \theta_{rmac}^{(T-20)}$	
B_{mac}^{total}		$\sum_{segments} \alpha_{mac} AB_{mac}$	
Dreissenids		$\frac{dB_{zm}}{dt}$	$(w_f I_{zm} - (w_f R_{zm} + w_f F_{zm} + w_f U_{zm})) B_{zm}$
		I_{zm}	$\alpha_{cr} B_{zm}^{b_r} \cdot f_I(t) \cdot \min\left(\frac{PP_w}{K_{cp}}, 1\right)$
	$f_I(t)$	$\frac{K_1 e^{\gamma_1(t-t_1)}}{1 + K_1 (e^{\gamma_1(t-t_1)} - 1)} \cdot \frac{K_4 e^{\gamma_2(t_4-t)}}{1 + K_4 (e^{\gamma_2(t_4-t)} - 1)}$	
	α_{cr}	$\alpha_c e^{-0.3z}$	
	γ_1	$\frac{1}{t_2 - t_1} \cdot \ln \frac{K_2(1-K_1)}{K_1(1-K_2)}$	
	γ_2	$\frac{1}{t_4 - t_3} \cdot \ln \frac{K_5(1-K_4)}{K_4(1-K_5)}$	
	R_{zm}	$\alpha_r \text{refill} B_{zm}^{b_r} \cdot f_r(t) + \frac{w_f}{W_r} \cdot SDA(I_{zm} - F_{zm})$	
	$\alpha_r \text{refill}$	$\alpha_r e^{-0.3z}$	
	$f_r(t)$	$v^x e^{x(1-v)}$	
	V	$\frac{t_m - t}{t_m - t_0}$	
	x	$\left(\frac{w(1 + \sqrt{1 + 40/y})}{20} \right)^2$	
	w	$\ln Q(t_m - t_0)$	
	y	$\ln Q(t_m - t_0 + 2)$	
	PP_w	$TP_w(1 - w_{DIP})$	
	F_{zm}	$\alpha_f \exp(\gamma_f \cdot \min\left(\frac{PP_w}{K_{cp}}, 1\right)) \cdot I_{zm}$	
U_{zm}	$\alpha_u(I_{zm} - F_{zm})$		
FR	$\frac{f_{max}}{K_{cp} \cdot 0.34}$ if $PP_w < K_{cp}$ $\frac{f_{max}}{PP_w \cdot 0.34}$ if $PP_w > K_{cp}$		
FT_{zm}	$FR B_{zm} \alpha_{zm} A_i N_{ab_i} PP_w$		
B_{zm}^{total}	$\sum_{i=1}^7 B_{zm_i} \alpha_{zm_i} A_i N_{ab_i}$		
Dissolved Inorganic Phosphorus	$\frac{dDIP_{sed}}{dt}$	$-D_{sed}(DIP_{sed} - DIP_w) + S_{sed}(DIP_{sede} - DIP_{sed}) + K_{decom} \cdot \frac{\rho}{\phi} \cdot OP_{sed} - G_{mac} \cdot \alpha_{mac} \cdot \left(\frac{A}{\phi V_{sed}}\right) \cdot B_{mac} \cdot BP_{mac}$	
	D_{sed}	$\theta_s^{T-20} \cdot \frac{K_{DO}}{K_{DO} + DO} \cdot \frac{\phi}{\delta^2} \cdot \frac{K_{diff}}{1 - \ln(\phi)}$	
	S_{sed}	ϕK_{ad}	
	DIP_{sede}	$\frac{PIP_{sed}}{E \cdot (PIP_{max} - PIP_{sed})}$	
Particulate Inorganic Phosphorus	K_{decom}	$K_{d20} \cdot \theta_s^{T-20}$	
	$\frac{dPIP_{sed}}{dt}$	$-f_{resus} \cdot \frac{A}{\rho V_{sed}} R_{resus} - S_{sed}(DIP_{sede} - DIP_{sed}) \cdot \frac{\rho}{\phi} - B_{sed-PIP} \cdot PIP_{sed}$	
Organic Phosphorus	B_{sed-pp}	$\frac{S_{pp}}{\phi}$	
	$\frac{dOP_{sed}}{dt}$	$\frac{V_s \cdot TP_w}{Z} \cdot \frac{A}{\rho V_{sed}} - (1 - f_{resus}) \cdot V_{sed} \cdot R_{resus} - B_{sed-pp} \cdot OP_{sed} - K_{decom} \cdot OP_{sed} + D_{mac} \cdot B_{mac} \cdot \frac{\alpha_{mac} \cdot A}{\rho V_{sed}} \cdot BP_{mac} + D_{zm} \cdot B_{zm} \cdot \frac{\alpha_{zm} \cdot A}{\rho V_{sed}} \cdot BP_{zm} + \frac{Psd_{f_{zm}}}{\rho V_{sed}}$	
Sediment resuspension	D_{zm}	$w_f \cdot (f_{OP} - ZM) \cdot U_{zm} + F_{zm}$	
	$Psd_{f_{zm}}$	$\alpha_{sed}(FT_{zm} - w_f \cdot I_{zm} \cdot A \cdot B_{zm} \cdot BP_{zm})$	
Inflows from the Main Basin to any of the inshore segments	R_{resus}	$\alpha_{sdr} \left(\frac{\tau - \tau_c}{\tau_c}\right)^{b_{sdr}}$ if $\tau \geq \tau_c$, 0 if $\tau < \tau_c$	
	$Q_{backflow}$	$(M_w + M_d) L_{segment}$	
Outflows from any inshore segment to the Main Basin	$Q_{outflow}$	$Q_{backflow} + Q_{trib}$	

(continued on next page)

Table 1 (continued)

Process	Symbol	Equation
Mw		$H_s^2 \sqrt{\frac{ng}{32}}$ where $\frac{gH_s}{U_a^2} = 0.0026 \left[\frac{gF}{U_a^2} \right]^{0.47}$ $t_d = \frac{0.0298 F}{I_s}$ $\frac{H_{ix}}{H_s} = \frac{8.98 \frac{I_s}{U_a}}{(1 + 7.95 \frac{I_s}{U_a})}$ $\frac{T_{ix}}{T_s} = \frac{4.35 \frac{I_s}{U_a}}{(1 + 3.35 \frac{I_s}{U_a})}$
Md		$\frac{U_s}{K} (1 - e^{-kz}),$ where $k = \frac{4.605}{D_{crit}}$ $D_{crit} = \frac{30.47 T_s}{\sin 2U_s}$ $\tau_s = (U_a^2 + 0.07U_a^3)10^{-4}$ $U_s = 0.035 U_a$

wind-induced wave propagation and current drifts controlled by the water surface shear stress (Tsanis, 1992). Wave movements were calculated based on the premise that the wave height is a function of wind speed, fetch and storm duration (Smith, 1979; see Table 1), while drift currents are assumed to follow the Ekman exponential decline of current speed with depth and are also driven by the Coriolis force (Smith, 1979). The bi-directional circulation patterns across the interface between the main basin and the two embayments meet equilibrium conditions by considering backflows that counterbalance the displaced volume of water (Baird & Associates, 2006; Tsanis, 1992).

2.2.2. Macrophyte submodel

The contribution of macrophytes to the phosphorus cycle is based on Asaeda et al.'s (2000) dry-mass biomass submodel, as recently modified by Kim et al. (2013). The model aims to reproduce the recent proliferation of submerged rooted plants in areas of 8–10 m deep due to the greater water transparency induced from the establishment of dreissenid mussels and external nutrient loading reduction (Ginn, 2011). The macrophyte governing equation considers: i) growth through uptake of segment-specific interstitial inorganic phosphorus content by their roots; ii) mortality representing the deposition of senesced plant tissues to the sediment organic phosphorus pool; and iii) the respiration through tubers to release P back to the water column. All biological processes are temperature-dependent based on the Arrhenius equation with maxima occurring during the summer stratified period. The growth term is also controlled by light availability with extinction coefficients reported by Depew et al. (2011b) and an average empirical depth of plant colonization (Ginn, 2011). The predicted macrophyte abundances (g dry weight or dw m⁻²) were converted to total P fluxes using literature-based segment-specific littoral areas of colonization (Depew et al., 2011a; Ginn, 2011) (Table 1), while the tissue phosphorus content is based on existing empirical estimates from Lake Simcoe (Depew et al., 2011b).

2.2.3. Dreissenid submodel

Our dreissenid submodel adopts the bioenergetic representation of the physiological activity of individual mussels (Bierman et al., 2005; Schneider, 1992). The dreissenid interaction with the water column and sediment layers depends on their filtration rates, food ingestion, respiration, excretion metabolism, production of faeces, pseudofeces, and dissolved P as end-products (Fig. 2). Filtering rate represents the volume of water swept clear of particles per unit time, which was modelled following Bierman et al.'s (2005) assumption that mussels maintain a maximum ingestion rate for all food concentrations below a saturation value and are negatively related to food abundance when this threshold is exceeded (Sprung and Rose, 1988). The capacity of dreissenid filtration to impact the entire water column is dependent upon the wind-induced turbulent mixing and the resultant eddy

diffusivity in the water column (Edwards et al., 2005). This process can suppress the dreissenid filtration effect on algae and other biogenic particles from littoral to pelagic zones, resulting in the formation of boundary layers near dreissenid mussel beds in stratified waters (Boegman et al., 2008). The latter effect is introduced in the model with a segment-specific and depth-dependent scaling clearance rate coefficient (Daunys et al., 2006). The rejected suspended solids and the remaining biodeposited particulate material are distributed between the water column and sediments (Fig. 2; Yu and Culver, 1999). The production rate of pseudo-feces is calculated as the difference between filtered and ingested food, assuming that the latter fraction corresponds to 34% of the filtered food (Walz, 1978). Counter to the Bierman et al. (2005) study, our approach does not explicitly consider age cohort classes, while the dynamics of individual dreissenid mussels are converted to an ecosystem-scale effect by multiplying the areal biomass estimates with a user-specified colonization area.

2.2.4. Sediment submodel

The model approximates the dynamic P transformation processes in the upper sediment layers with an active P pool (OP_{sed}, PIP_{sed}, and DIP_{sed}) constrained by measured data by Ditttrich et al. (2013). The sediment accumulation depths in most model segments extend beyond the simulation time period of 9 years (1999–2007) with 10 years of sediment accumulation history in Cook's Bay, 22 years in Kempenfelt Bay, and 36 years in the main basin (Hiriart-Baer et al., 2011). Being the residues of algae, macrophyte dead tissues, and dreissenid egested/excreted material, organic P is transported towards the deeper sediments through burial. Temperature-dependent biological decomposition of organic P in the sediments leads to the regeneration of dissolved phase P. Dissolved P is subjected to diffusion and adsorption-desorption to/from the sediment particles. Following Hiriart-Baer et al.'s (2011) findings, the sediment burial of particulate fractions (OP_{sed} and PIP_{sed}) was assumed to be the lowest in the main basin and the highest in Cook's Bay. We use Michaelis-Menten kinetics and the Arrhenius equation to describe the release rate of dissolved P from the surface layer into the overlying water as a function of the concentration gradients, the dissolved oxygen availability and temperature. Exchangeable particulate P may act as a sink or source, depending on the difference between the concentration in interstitial waters and a dynamic equilibrium concentration of dissolved P. The latter concentration was estimated from the exchangeable particulate P in sediments, assuming non-linear sorption partitioning described by the Langmuir isotherm (Wang et al., 2003a,b). Sediment resuspension is another potentially important sink of the sediment P pool that depends strongly upon the magnitude of the bottom shear stress (Lick, 1986; Mehta et al., 1982; Tsai and Lick, 1986). Similar to Kim et al. (2013), we used an empirical expression that postulates a linear relationship between sediment resuspension rate and the excess bed shear stress (Chao

et al., 2008; Mehta et al., 1982). The bottom shear stress associated with the near-bed wave velocity was assumed to be much larger than that associated with the near-bed current velocity (Mian and Yanful, 2004). The Sverdrup–Munk–Bretschneider (SMB) method for shallow water bodies was then used to quantify the bed shear stresses, as a function of the wave characteristics (height, period length), the water depth, the wind speed and fetch length (CERC, 1994).

The model was manually calibrated to reproduce the average TP dynamics in the system and subsequently validated by focusing on its capacity to reproduce the year-to-year variability during the study period 1999–2007 (Table 2). The philosophy underlying this strategy was articulated in several recent papers (Arhonditsis and Brett, 2005; Gudimov et al., 2011). It should also be noted that because our dataset does not contain any information from the period that the system was eutrophic, i.e., all the years represented more or less the current mesotrophic conditions prevailing in the system, we are unable to fully evaluate the capacity of the ecosystem characterization presented herein to support predictions in the extrapolation model domain. We used the average error (AE), the relative error (RE), and the root mean square error (RMSE) to estimate the agreement of the daily TP predictions with the corresponding observed values (Stow et al., 2003). Sensitivity analysis was conducted to quantify the dependence of model predictions on model inputs. Specifically, we reported the 95% predictive intervals associated with the uncertainty of the exogenous TP loading and hydrodynamic inter-segment exchanges (Table 3). These forcing functions were treated stochastically, using Latin Hypercube sampling; namely, each input was sampled independently from a uniform distribution based on a coefficient of variation that reflected the corresponding observed variability, i.e., 15–50% in this study. Additionally, the sensitivity of model endpoints to parameters related to the dynamics of macrophytes, dreissenids or sediment P release was tested by inducing perturbations to the values assigned during the calibration exercise. The range of these perturbations was roughly based on Omlin et al.'s (2001) uncertainty classification scheme of accurately (<5–10%), moderately (15–25%), and poorly (50%) known model parameters.

3. Results

The comparison between the observed and predicted TP concentrations in the different model segments is illustrated in Fig. 3, while the associated fit statistics are provided in Table 4. The fit statistics are on par with the error values reported for other TP mass-balance models developed in the Great Lakes (Chapra and Dolan, 2012). The RMSE values varied from 4.5 to 6.5 $\mu\text{g TP L}^{-1}$ for daily concentrations and 2.5 to 4.1 $\mu\text{g TP L}^{-1}$ for seasonal mean values. The RE values ranged from 32 to 37% and 11 to 23% for daily and seasonal TP concentrations, respectively. The TP concentrations are overestimated in the main basin and the East End of Lake Simcoe with AE of 1.2–2.4 $\mu\text{g TP L}^{-1}$, but they are underestimated in Cook's Bay with a negative AE ($\approx -1.7 \mu\text{g TP L}^{-1}$). Interestingly, our sensitivity analysis showed that both exogenous P loading and hydrodynamic forcing can induce significant variability in the two embayments, whereby conditions of long residence time and increased nutrient inflows result in simulated TP levels of 40–50 $\mu\text{g L}^{-1}$ in Cook's Bay and 20–30 $\mu\text{g L}^{-1}$ in Kempenfelt Bay. The present model provided improved fit to the observed TP patterns in Cook's Bay relative to Gudimov et al.'s (2012) continuous stirred-tank reactor (CSTR) model, as the RMSE values decreased from 10.8 to 6.4 $\mu\text{g TP L}^{-1}$. In the main basin, the RMSE values remained practically unaltered ($\approx 4.0\text{--}4.5 \mu\text{g TP L}^{-1}$) while the fit in Kempenfelt Bay worsened from 3.2 to 5.7 $\mu\text{g TP L}^{-1}$.

Similar to Gudimov et al.'s (2012) results, our model appears to downplay the intra-annual TP dynamics, indicative of a more complex interplay among exogenous loading, hydrodynamics and biological productivity that most likely modulates in-lake TP variability. In particular, the first feature of the current model that disallows capturing the within-year variability of the system has to do with its coarse spatial resolution and thus limited ability to depict the hydrodynamic interplay between inshore and offshore locations as well as the pollutant dynamics in the latter segments. Given the lack of information to support the implementation of an explicit 2D or 3D hydrodynamic model, we had to adopt a spatial model configuration that mainly serves the purpose of evaluating the potential of exogenous phosphorus loads

Table 2
Calibration parameters for Lake Simcoe TP model.

Symbol	Variables and Parameters	Value	Units
K_{d20}	Decomposition rate coefficients at 20 °C		
	Kempenfelt Bay epilimnion	0.0025	day ⁻¹
	Kempenfelt Bay hypolimnion	0.00075	
	Cook's Bay epilimnion	0.0078	
	Cook's Bay hypolimnion	0.0006	
	East End epilimnion	0.0006	
	Main Basin epilimnion	0.00065	
	Main Basin hypolimnion	0.00013	
D_{mac}	Macrophyte mortality rate	0.001	
K_p	Half saturation constant for phosphate in sediment pore water	5	$\mu\text{g L}^{-1}$
PIP_{max}	Maximum sorption capacity		
	Kempenfelt Bay epilimnion	1.0	mg g ⁻¹
	Kempenfelt Bay hypolimnion	1.0	
	Cook's Bay epilimnion	0.4	
	Cook's Bay hypolimnion	0.4	
	East End epilimnion	0.8	
	Main Basin epilimnion	0.8	
	Main Basin hypolimnion		
P_m	Maximum gross photosynthesis rate	0.030	
R_{mac20}	Macrophyte respiration rate at 20°C	0.018	day ⁻¹
$V_s\text{-chla}$	Settling rate of phytoplankton	0.005	m day ⁻¹
$V_s\text{-pp}$	Settling rate of organic matter other than phytoplankton	0.020	m day ⁻¹
α_2	Phytoplankton self shading effect	0.02	m ² mg chla ⁻¹
FR	Dreissenid filtration rate	500/350–500 ^a	mL ind ⁻¹ day ⁻¹
	Dreissenid filtration rate	23/20.9–30.2 ^a	mL ind ⁻¹ hr ⁻¹
B_{zm}	Individual weight of a dreissenid mussel	14 ^a	mg WW ind ⁻¹
L_{zm}	Length of an individual dreissenid	11/5–24.6 ^b	mm ind ⁻¹
α_{sdr}	Resuspension coefficient	2	mg P m ² day ⁻¹

a (Ozersky et al. 2013)

b (Evans et al. 2011)

Table 3
Forcing functions of exogenous loading, intersegment flow/mass exchanges, and model estimates of P settling fluxes.

TP mass balance model										
Segment	TP load tonnes P yr ⁻¹ min-max (CV)	Flow, x10 ⁶ m ³ day ⁻¹ min-max (CV)	Settling velocity m yr ⁻¹	TP export, tonnes P yr ⁻¹	Settling flux from epilimnion, mg P m ⁻² yr ⁻¹	Segment	TP load tonnes P yr ⁻¹	Settling velocity, m yr ⁻¹	TP export, tonnes P yr ⁻¹	Settling flux from epilimnion, mg P m ⁻² yr ⁻¹
Cook's Bay	12.1–24.5 (17%)	1.6–18.2 (42%)	6.6	13.1	51	C1	16.1	2.0	15.3	62
						C6	2.3	52.1	4.2	976
						C9	2.2	6.6	3.4	94
Kempenfelt Bay	7.4–11.2 10%	2.3–23.5 (41%)	6.5	7.3	51	K39	8.3	33.5	3.8	491
						K42	1.4	6.2	3.0	83
East End	14.4–25.6 (14%)	8.1–107.0 (43%)	6.6	6.4	124	East End	21.9	6.2	4.2	72
Main basin	15.6–27.8 (14%)	-	6.5	12.1	71	S15	7.0	3.6	3.3	44
						K45	15.5	6.9	9.6	83

to shape the macrophyte community and dreissenid mussels, under the typical residence times experienced in the embayments of Lake Simcoe. Another major issue is associated with the phosphorus loading estimates, which are based on linear interpolation of semi-monthly measurements of stream flow and phosphorus concentrations in most of the tributaries. As such, the model is forced primarily with baseflow conditions, whereas the hydrological regimes induced by extreme precipitation events are somewhat under-represented. These two factors alone can be responsible for the more static behaviour of our model and its tendency “to predict annual average concentrations and ignore short term phenomena (e.g., seiche effects) and seasonal variability” (Maccoux et al., 2013).

The specification of the settling velocities in the different model segments is provided in Table 2. The average TP settling rate of 6.5 m yr⁻¹ falls within the 4–13 m yr⁻¹ range reported for mesotrophic embayments in Lake Superior (Chapra and Dolan, 2012). The annual settling velocities are also comparable with those derived by the CSTR model with the highest rate in Cook's Bay and the lowest in the main basin (Gudimov et al., 2012). According to our model, the amount of P exported from the main basin through the outlet in Atherley Narrows was estimated to be 12.1 tonnes P yr⁻¹, which falls within the typically reported range of 6.9–14.3 tonnes P yr⁻¹ and corresponds to an average of 83% P retention in Lake Simcoe (LSRCA and MOE, 2006, 2012). The net export of 13.1 tonnes P yr⁻¹ from Cook's Bay to the main basin is distinctly higher from Gudimov et al.'s (2012) estimate of 3.4 tonnes P yr⁻¹, but the latter model also predicted an elevated epilimnetic loss of 13.1 tonnes P yr⁻¹ at the middle area of the embayment (Gudimov et al., 2012). Likewise, the net export of 7.3 tonnes P yr⁻¹ from Kempenfelt Bay is higher than Gudimov et al.'s (2012) net export of 3.0 tonnes P yr⁻¹, and instead the CSTR model suggested an elevated loss of 4.5 tonnes P yr⁻¹ at the inner segment of this embayment (segment K39; Fig. 1). The explicit consideration of macrophytes and dreissenids modified significantly the P sedimentation fluxes reported by Gudimov et al. (2012) in Cook's Bay (62–976 versus 51 mg P m⁻² yr⁻¹), Kempenfelt Bay (83–496 versus 50.6 mg P m⁻² yr⁻¹), and East End (72 versus 124 mg P m⁻² yr⁻¹), while the main basin remained mostly unaffected (44–83 versus 71 mg P m⁻² yr⁻¹).

Segment-specific model predictions and measured values for aquatic macrophytes, dreissenids, and sediments are also provided in Table 5. Our model predicts that the end of summer macrophyte biomass can reach values up to 120 g dw m⁻² in the Cook's Bay epilimnion and 100 g dw m⁻² at the littoral zone of the East End, which correspond to annual average values of ≈75 and 70 g dw m⁻², respectively. These predictions are on par with the empirical estimates of 60–80 g dw m⁻² reported for the nearshore areas in the middle and outer Cook's Bay, but underestimate the biomass values (>80 g dw m⁻²) at the innermost sites of this embayment (Ginn, 2011). The reason for the discrepancy in the inner Cook's Bay is that our model predicts a severe macrophyte limitation stemming from the nutrient availability in the interstitial waters of the top sediment layer, which in turn represents the accumulation history over the last 10 years. The annual P loading in Cook's Bay has dramatically fallen from 70 tonnes P yr⁻¹ in 1990–1991 to an approximate average of 20 tonnes P yr⁻¹ during the 1998–2008 period. Thus, higher macrophyte biomass values could be achieved by considering higher “legacy P” stored in the deeper sediments during the eutrophic past (see Fig. 4 ESM), especially directly at the outlet from Holland Marsh dykes where most of the terrestrial P load settles down (Depew et al., 2011a). The model also overestimates somewhat the observed macrophyte abundance in the nearshore sites of Kempenfelt Bay and the main basin, 20–40 g dw m⁻². Our model postulates that the metabolic by-products excreted through respiration represent a direct gain for the TP pool in the water column, and therefore the macrophyte parameter specification could partly drive the model predictions (Figs. 1–3 ESM). The scenario of light deficiency for macrophytes in Cook's Bay and East End results in a decrease by

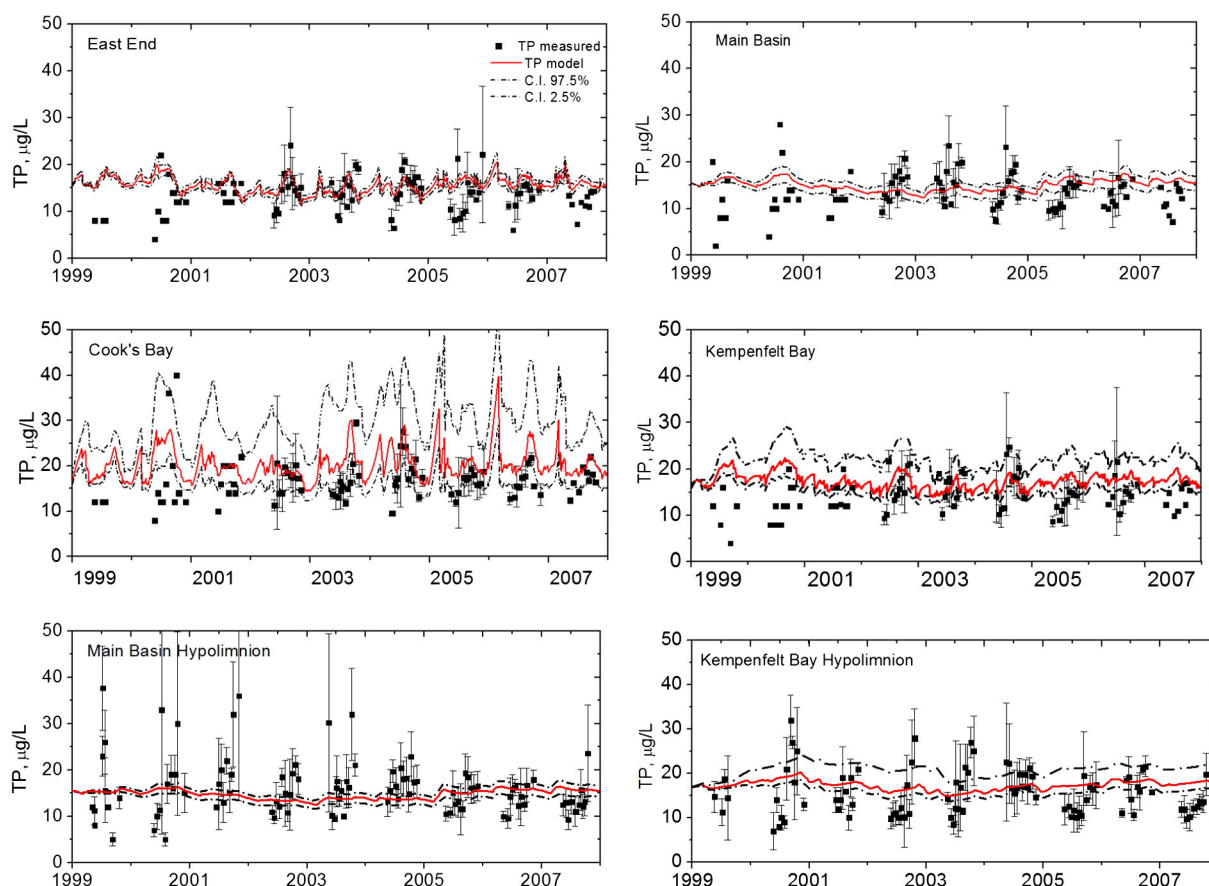


Fig. 3. Model fit with 95% uncertainty bounds related to the error in the characterization of the TP loading and hydraulic intersegment exchanges.

1–2 $\mu\text{g TP L}^{-1}$ (Fig. 1 ESM; lines A), while the opposite holds true for the scenario of optimal illumination (Fig. 1 ESM; lines B), except from Cook's Bay in which DIP_{sed} is the predominant limiting factor. Similar to Kim et al.'s (2013) findings, the TP increase with the scenario of optimal illumination of the water column can be offset by assigning a higher value to the optimal solar radiation for macrophyte growth (Fig. 1 ESM; lines C). Model sensitivity to the specification of the macrophyte DIP_{sed} affinity is comparable with the light limitation effects (Fig. 2 ESM). Similar influence on the water column TP concentrations can be obtained by the values assigned to macrophyte growth, metabolic losses, and sediment mineralization rates, i.e., faster macrophyte growth and metabolic rate coupled with active sediment decomposition can shift up the ambient levels by 1.5–2.0 $\mu\text{g TP L}^{-1}$ relative to the reference conditions (Fig. 3 ESM; lines A–C).

The model parameter specification reflects the filtration behaviour of individual dreissenid mussels of an average size of 11 mm, which falls within the reported range of 5–24.6 mm ind^{-1} (Ozersky et al.,

2013). The simulated mussel clearance rate of 23 $\text{mL ind}^{-1} \text{h}^{-1}$ ($1.2\text{--}7.5 \text{ L g}^{-1}$ shell-free dry mass or SFDM h^{-1}) falls within the reported range of $20.9 \pm 30.2 \text{ mL ind}^{-1} \text{h}^{-1}$ ($3.6 \pm 4.7 \text{ L g}^{-1} \text{ SFDM h}^{-1}$) (Ozersky et al., 2013). Taking into account the dreissenid area distribution reported by Ozersky et al. (2011) along with a whole-lake average population density of 7000 in. m^{-2} (Evans et al., 2011), the model predicts a total dreissenid biomass of $12 \cdot 10^3$ tonnes SFDM; $11.9 \cdot 10^3$ tonnes SFDM in Ozersky et al. (2011). This predicted biomass in turn corresponds to a nominal areal grazing rate of 2.6–3.8 $\text{m}^3 \text{ m}^{-2} \text{ day}^{-1}$, which is comparable to the empirical estimate of 0.2–6.4 $\text{m}^3 \text{ m}^{-2} \text{ day}^{-1}$ in Lake Simcoe (Schwalb et al., 2013). If nominal clearance rates are taken into account, the whole lake volume can be filtered every ten days (Ozersky et al., 2013), based on Coughlan's (1969) assumption that the suspended particles are homogeneously mixed with dreissenids having access to the whole water volume and the filtered particles are permanently deposited and thus not filtered again. Nonetheless, our model does not support such extreme predictions about the role of the dreissenids, as we postulate a reduced clearance rate due to refiltration of suspended particles (i.e., 71–86% of the inhaled water is refiltered), reflecting the limited effect of turbulence in the water column mixing as well as the refiltration due to high dreissenid density (Yu and Culver, 1999). The model also approximately mimics the formation of a boundary layer in areas below the mixed layer (>8 m deep), where dreissenids have access mostly to particles settled from the epilimnion (Boegman et al., 2008), as the predictions of a filtered TP of ~60 tonnes P yr^{-1} far exceed the epilimnetic fluxes of ~40 tonnes P yr^{-1} settling in the hypolimnion of the main basin (Fig. 4).

Sensitivity analysis of the dreissenid submodel shows ambient TP increases by 5–8 $\mu\text{g TP L}^{-1}$ in response to dreissenid low density population of 1000 in. m^{-2} (e.g., 3.5 g SFDM m^{-2} at the East End

Table 4

Goodness-of-fit statistics for TP predictions based on root-mean-squared error (RMSE), average error (AE), relative error (RE) and coefficient of determination (r^2).

Model segment	RMSE $\mu\text{g P/L}$	AE $\mu\text{g P/L}$	RE %	r^2 ^c
Cook's Bay	6.4 ^a /3.0 ^b	−1.7/2.5 ^b	32/11 ^b	0.47/0.94
Kempenfelt Bay	5.7/4.1	2.9/3.0	37/23	0.34/0.90
East End	4.7/2.9	2.4/2.4	36/19	0.38/0.78
Main basin	4.5/2.5	1.2/1.2	32/16	0.12/0.81

^a Daily TP predictions.

^b Summer stratified average TP values.

^c Summer stratified annual average/maximum value for a specific year.

Table 5
Model predictions and measured values for aquatic macrophytes, dreissenids, and sediments.

Segment/Model endpoint	Cook's Bay		Kempfenfelt Bay		East End		Main basin		Total	
	Model	Obs.	Model	Obs.	Model	Obs.	Model	Obs.	Model	Obs.
Macrophytes abundance	35–116	75	21–67	20–40	32–95	70	32–95	20–40	–	–
Macrophytes colonization area, km ²	17.8	17.8	1.5	NA	24.9	NA	11.6	NA	56	56
Macrophytes biomass, tonnes dw	1000	NA	58	NA	1500	NA	700	NA	3300	NA
Macrophytes P content	2800	1169 ^a	120	NA	3600	NA	1500	NA	8000	NA
Dreissenids biomass, tonnes SFDM	600	450	200	200	3200	3600	7000	7400	11,000	11,500
Sediment OP (fast degradable) accumulation mg P g dw ⁻¹	0.11	0.12	0.25	0.22	NA	NA	0.14	0.17	–	–
Flux from sediments, mg P m ⁻² day ⁻¹	0.07–0.11	0.10	0.18–0.21	0.20	0.07–0.08	NA	0.07–0.08	0.07	–	–

^a Estimated in 1988 under eutrophic conditions.

compared to 22 g SFDM m⁻² under the reference conditions), whereas an increased abundance of 10,000 in. m⁻² (or 33 g SFDM m⁻²) results in a decrease by 2–3 µg TP L⁻¹ depending on the embayment considered (Fig. 4 ESM). Interestingly, the characterization of the dreissenid ingestion and metabolic strategies does not appear to be particularly influential to the TP model predictions (Fig. 5 ESM). Finally, we note that the modelled dreissenid P excretion rate is 4.0 µg P g⁻¹ SFDM day⁻¹, which falls within the [Ozersky et al.'s \(2013\)](#) estimate of 1.6–12.8 µg P g⁻¹ SFDM day⁻¹.

The sediment submodel predictions are the result of a complex dynamic equilibrium among P in the water column, macrophytes, dreissenid mussel activity and sediment processes. The model predictions for sediment organic P closely match the measured concentration profile of organic bound P fraction at stations K45, K42 and C9, as represented by the NaOH-NRP fraction under the sequential P fractionation schema reported by [Dittrich et al. \(2013\)](#). The model predicts segment-specific concentrations of 0.11 mg P g⁻¹ dw at station C9 in Cook's Bay (compared to a measured active pool of 0.12 mg P g⁻¹ dw), 0.25 mg P g⁻¹ dw at station K42 in Kempfenfelt Bay (measured value of 0.22 mg P g⁻¹ dw) and 0.14 mg P g⁻¹ dw at station K45 in the main basin (compared to 0.17 mg P g⁻¹ dw). The modelled sediment diffusive fluxes are in complete agreement with the values reported by [McCulloch et al. \(2013\)](#), i.e., 0.1 mg P m⁻² day⁻¹ at station C9, 0.2 mg P m⁻² day⁻¹ at K42, and 0.07 mg P m⁻² day⁻¹ at K45. According to our sensitivity analysis, the value assigned to the sediment porosity moderately affects the water column TP concentrations (<2 µg L⁻¹) (Fig. 6 ESM). In a similar manner, shifting the sediment characterization towards the predominance of adsorption or desorption processes can vary the ambient TP levels by 2–4 µg L⁻¹ (Fig. 7 ESM). Finally, our model demonstrates low dependence on the parameters related to P diffusive fluxes; namely, the diffusion coefficient and sediment thickness. This limited response can be potentially enhanced if we consider the legacy TP in the deeper sediments, which requires consideration of non-steady-state behaviour and complete accumulation history.

Based on the model parameter specification, the various external and internal TP flux rates in Lake Simcoe are presented in Fig. 4 and Table 6. The net TP contributions (sources or sinks) represent the mass of P associated with the various compartments (water column, sediments, macrophytes, dreissenids) averaged over the 1999–2007 period. In Cook's Bay, the P budget is predominantly driven by the external sources (P loading: 18.3 tonnes P yr⁻¹) and sinks (outflow: 13.1 tonnes P yr⁻¹). Dreissenids approximately filter 68.5 tonnes P yr⁻¹ from the water column and subsequently egest 58.5 tonnes P yr⁻¹ via their metabolic excretion and particle rejection, whereas an additional 6.7 tonnes P yr⁻¹ of pseudofeces is deposited onto the sediments. Interestingly, our model suggests that the sediments (resuspension and diffusion from the sediments to water column minus particle settling) act as a net sink in this segment (2.7 and 1.2 tonnes P yr⁻¹ in the epilimnion and hypolimnion, respectively). Likewise, the macrophyte intake of P from the interstitial waters is responsible for a net loss of 8.6 tonnes P yr⁻¹ from the sediments, and

an approximately equal amount is returned into the water column through respiration/excretion. In a similar manner, the macrophyte uptake minus the amount of P regenerated from the decomposition of the dead plant tissues can take away 12.7 tonnes P yr⁻¹ from the sediments in the eastern part of Lake Simcoe, while the subsequent release of their metabolic by-products is responsible for 12.8 tonnes P yr⁻¹. The particulate P settling clearly dominates over the resuspension and diffusion from the sediments to the water column with the corresponding net fluxes being equal to 5.8 tonnes P yr⁻¹. Kempfenfelt Bay receives 9.3 tonnes P yr⁻¹ from exogenous sources, while 7.3 tonnes P yr⁻¹ is transported into the main basin. The total net loss to the sediments accounts for 1.6 tonnes P yr⁻¹, while dreissenids on average reduce the ambient TP levels by 0.8 tonnes P yr⁻¹. In the main basin, the dreissenids filter 103.1 tonnes P yr⁻¹ and approximately 90% of that amount (93.5 tonnes P yr⁻¹) is returned into the water column as pseudofeces or other metabolic excreta. In the same area, external P loading accounts for about 21.7 tonnes P yr⁻¹, while an average of 12.1 tonnes P yr⁻¹ is exported through the outflow into Lake Couchiching. Our model postulates that the burial into the deeper sediment layers of the main basin (including its east end) represents a significant pathway (15.6–39.1 tonnes P yr⁻¹) through which P is essentially lost from the system.

4. Discussion

In the context of eutrophication modelling, [Gudimov et al. \(2012\)](#) cautioned that the recent trend to increase model complexity, without ensuring that commensurate empirical knowledge from the studied system exists, can compromise our ability to effectively constrain parameters from observations. As a result of this practice, the inflated uncertainty undermines model credibility for supporting environmental management decisions. For this reason, the same study advocated the use of simple models as adequate first-order approximations until simplicity can be gradually traded for increased explanatory power ([Gudimov et al., 2012](#)). However, [Kim et al. \(2013\)](#) argued that the conventional P mass-balance (e.g., Vollenweider-type) models are structurally inadequate to represent one of the most critical facets of eutrophication, i.e., the causal linkage among external loading, internal recycling and summer ambient concentrations. In Lake Simcoe, recent empirical evidence has made it abundantly clear that the complex interplay among macrophytes, dreissenids and sediment diagenesis appears to modulate the TP dynamics in the system. From a management standpoint, the presence of a significant positive feedback loop could suggest a disconnect between external loading and ambient nutrient levels, and thus the anticipated water quality improvements by additional exogenous nutrient loading reductions may not be realized within a reasonable time frame. By invoking extra complexity, the present model structure offered the opportunity to examine (and potentially shed light) on the role of different nutrient recycling pathways.

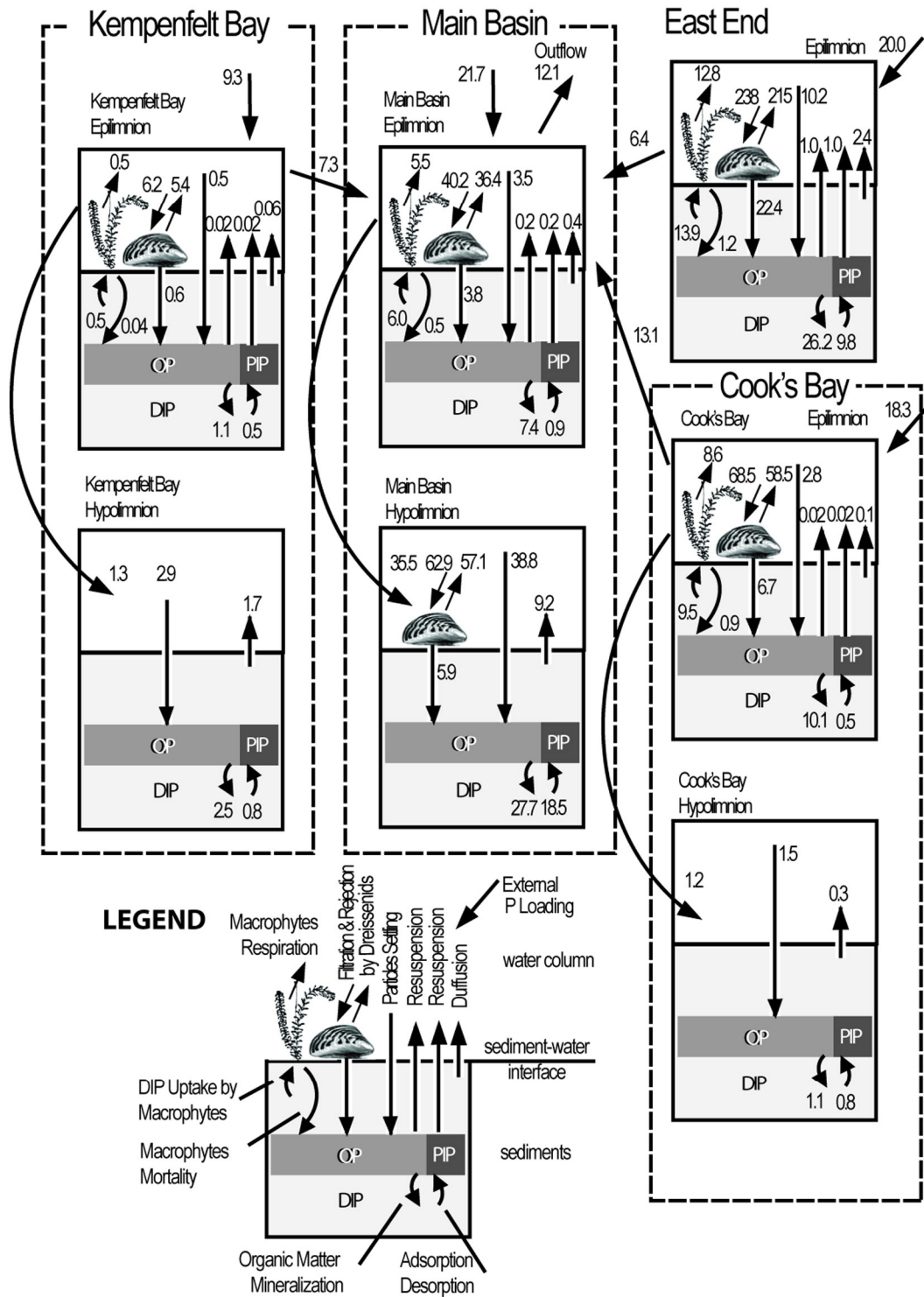


Fig. 4. Simulated phosphorus fluxes (tonnes P yr⁻¹) in water column and sediment layer in the four spatial segments of Lake Simcoe.

4.1. What is the influence of macrophytes on the phosphorus cycling in Lake Simcoe?

The macrophyte community in Lake Simcoe is currently dominated by *Ceratophyllum demersum* (39.1% of the total biomass), the invasive species *Myriophyllum spicatum* (27.4%), *Elodea canadensis* (10.7%) and *Chara* spp. (9.7%) (Ginn, 2011). The controlling factors of the submerged macrophyte distribution and abundance are the depth, the fetch/wave exposure, the sediment texture and stability, and the P loading from

the closest tributary along with the size of the area drained (Ginn, 2011). A nearly threefold increase in aquatic plant biomass has been recorded since 1984, with macrophytes proliferating into much deeper (from 6.0 m in 1984 to 10.5 m in 2008) waters with increasing water clarity (Ginn, 2011). Several mechanisms have been proposed to determine the role of aquatic macrophytes as either nutrient sources or sinks in the surrounding water (Barko and James, 1998; Bini et al., 2010; Christensen, 1999; Eriksson and Weisner, 1999; Sand-Jensen, 1998; Wigand et al., 1997; Zimmer et al., 2001). Submerged macrophytes

obtain P both from the water column and the sediment substrate, but under normal pore and ambient P concentrations, nutrient intake from the sediments dominates. In doing so, they can provide a significant pathway for the rapid transport of the nutrients assimilated from the sediments into the water column; a process known as “nutrient pump effect” (Asaeda et al., 2000; Howard-Williams and Allanson, 1981). Macrophytes also demonstrate high luxury uptake capacity and tend to accumulate nutrients in levels higher than their physiological requirements, and therefore the decomposition of dead plant tissues may be an important source of nutrients (Bini et al., 2010). Productive macrophyte stands could also cause hypoxia at night-time, thereby increasing sediment P fluxes (Bini et al., 2010), but even in well-oxygenated water, the increased photosynthetic rates elevate water pH (>9), which can similarly accelerate P release from the sediments (Barko and James, 1998). Nonetheless, there is another suite of mechanisms that can potentially minimize the P release from decaying macrophytes, such as foliar absorption or rapid phytoplankton uptake, and thus their presence may not always be positively related to the ambient nutrient concentrations (Rørslett et al., 1986).

In accordance with empirical evidence, our model consistently predicts that macrophyte intake from the interstitial waters is responsible for a significant loss of P from the sediments. For example, in Cook's Bay, Johnson and Nicholls (1989) found a sediment TP $\approx 1040 \mu\text{g g}^{-1}$ relative to a recently reported mean value of $518 \mu\text{g g}^{-1}$, with $\approx 300 \mu\text{g g}^{-1}$ in the southern area of this embayment where the highest plant biomass was recorded (Ginn, 2011). Our study also postulates that approximately equal P mass was returned into the water column as metabolic excreta. The latter characterization presumably deviates from the notion that the release of sediment-derived P from actively growing macrophytes is of minor importance compared to the quantities of nutrients released during macrophyte decay (Rørslett et al., 1986). In this study, there are two basic reasons why we opted for a parameter specification that likely overstates the direct P release from macrophytes relative to the indirect path of the bacteria-mediated decomposition of dead plant tissues on the sediments: (i) it makes it easier to “partial out” the influence of macrophytes on the P cycling in the water column, given the simplified mathematical description of the actual nature of the processes associated with the breakdown of the fallen litter (e.g., dependence on the content of structural carbohydrates and nutrients); and (ii) it facilitates the reproduction of the ambient TP levels in Lake Simcoe during our calibration exercise. In particular, depending on the macrophyte characterization as *r* or *K* strategists (i.e., organisms with faster/slower growth and metabolic rates) combined with fast or slow sediment decomposition rates, the macrophyte activity can vary the ambient TP levels by 2.0–4.0 $\mu\text{g L}^{-1}$.

4.2. How critical is the role of the phosphorus fluxes associated with the dreissenid mussels in Lake Simcoe?

In Lake Simcoe, according to Ozersky et al.'s (2011) survey, 3.5% of the total dreissenid biomass (≈ 12 tonnes SFDM) is found in Cook's Bay. In Kempenfelt Bay and the main basin, more than 25% of total dreissenid biomass was estimated to be in the 0–3.5 m depth interval, $\approx 32\%$ of dreissenid biomass in the 3.5–8 m depth interval, and only a minor proportion of dreissenids can be found at depths greater than 20 m (see Fig. 1 in Schwalb et al., 2013). Our model predicts that dreissenids filter a considerable amount of particulate P from the water column (6.2–238 tonnes P yr^{-1}), but the effective clearance rate is significantly lower (0.8–22.8 tonnes P yr^{-1}) with a substantial amount of the filtered particles (>85%) returned into the water column as faeces, pseudofeces or other metabolic excreta. The latter finding is not surprising as the ratio between zebra mussel filtration and effective clearance rate can vary between 3.4 and 6.9 (Yu and Culver, 1999). In particular, our model highlights the critical role of dreissenids in the shallow eastern end of Lake Simcoe, where they filter 238.5 tonnes P yr^{-1} from the water column and subsequently egest 215.0 tonnes P yr^{-1} , while an additional 22.4 tonnes P yr^{-1} of metabolic excreta is deposited onto the sediments. Because of its shallow morphology, a large portion of the eastern area is located within the euphotic and well-mixed zone, and therefore the elevated benthic photosynthesis and access of the dreissenids to sestonic algae create favourable conditions for biodeposition and nutrient recycling (Ozersky et al., 2013). Importantly, the large fetch of Lake Simcoe, the relatively deep epilimnion, and the fairly rapid horizontal mixing often induce hydrodynamic conditions that may allow the localized impacts of dreissenids to shape ecosystem-scale patterns (Schwalb et al., 2013).

In a recent synthesis paper, North (2013) provided evidence that six out of eleven predicted effects of the nearshore P shunt hypothesis are supported by the long-term patterns in Lake Simcoe (Higgins and Vander Zanden, 2010). For example, littoral benthic invertebrates on hard substrates have increased in abundance and diversity (Ozersky et al., 2011), while the biomass of non-dreissenid profundal benthic invertebrates decreased (Jimenez et al., 2011; Rennie and Evans, 2012). Counter to the expected responses, though, there was no evident change in the ice-free P concentrations, phytoplankton biovolumes and relative abundance of filamentous benthic algae. North (2013) attributed the lack of declining P concentrations to the year-to-year variability of the exogenous P loading prevailing over the nearshore dreissenid filtration effects. Given the current mesotrophic state of Lake Simcoe, it is not unreasonable to postulate a stronger reliance of the ambient P dynamics upon the external nutrient subsidies. However, our modelling analysis suggests that the presence of active nutrient recycling pathways, potentially magnified by the particular

Table 6

TP fluxes (tonnes P yr^{-1}) from different mechanisms considered by the model under the characterization of the sediment P release as per Dittrich et al. (2013).

Site	water-sed	water-mac	water-ZM	sed-ZM	sed-mac	Burial	Water in	Water out
KBe	−0.4	0.5	−0.8	0.6	−0.5	0.6	9.3	7.3
KBh	−1.2	0.0	0.0	0.0	0.0	1.3	0.0	0.0
CBe	−2.7	8.6	−10.0	6.7	−8.6	0.7	18.3	13.1
CBh	−1.2	0.0	0.0	0.0	0.0	1.2	0.0	0.0
E1	−5.8	12.8	−22.8	22.4	−12.7	15.6	20.0	6.4
MBe	−2.7	5.5	−3.8	3.8	−5.5	1.0	21.7	12.1
MBh	−29.6	0.0	−5.8	5.9	0.0	39.1	0.0	0.0

•water-sed: (resuspension and diffusion from the sediments to water column) − (particle settling).

•water-mac: (macrophyte respiration).

•water-ZM: (respiration, $0.4 \times$ excretion and refiltration rejection of dreissenids) − (particle filtration of dreissenids).

•sed-ZM: $0.6 \times$ excretion, egestion and direct rejection to sediments from dreissenids.

•sed-mac: (macrophyte mortality) − (macrophyte intake from sediment).

•Burial: burial rate into deeper layers.

•Water in: upstream inflow and external loading.

•Water out: downstream outflow.

morphological features and hydrodynamic patterns of Lake Simcoe, could alleviate the direct effects of dreissenid filtration and therefore the system has not experienced distinct decreasing trends in regard to its P levels.

4.3. What is our contemporary understanding of the role of the sediments?

The sediment submodel is an adaptation of the McCulloch et al. (2013) dynamic reactive-transport model, based on the calibration dataset derived from Dittrich et al. (2013) sediment core analysis. From a management point of view, the primary interest is to estimate how P loading into the different basins will impact the local net P sedimentation (or retention) rates and consequently the Lake Simcoe water quality. For example, using the characterization of the P cycle presented in Fig. 4, we can calculate the retention capacity in Cook's Bay to be about 28%, which is fairly close to Dittrich et al.'s (2013) value of 36% but significantly lower than Johnson and Nicholls' (1989) estimate of 48% in the 1980s. Thus, the colonization of the embayment by dreissenids and the recent proliferation of macrophytes appear to render support to Dittrich et al.'s (2013) hypothesis that the P retention in Cook's Bay may have decreased. The predominant fraction of TP is carbonate-bound P (apatite-P) mainly due to the accelerated erosion in the catchment. Furthermore, the TP content in the sediments of Cook's Bay is the lowest among the three studied basins in Lake Simcoe, providing evidence that the high sedimentation rates and natural watershed sources may lead to a "dilution" of P in the sediment dry matter. In contrast, Kempenfelt Bay typically received half of the external P loading that Cook's Bay received, yet the model predicts a P retention of 22% (2.0 tonnes P yr⁻¹), which is very similar to the 25% estimate in the 1980s (Johnson and Nichols, 1989) but much lower than Dittrich et al.'s (2013) sedimentation rate (≈70%). In the same segment, though, the hypolimnetic sediments were responsible for a fairly high diffusive P flux into the water column (≈1.7 tonnes P yr⁻¹), presumably reflecting the highest proportion of the redox-sensitive P sediment pool compared to other lake segments as well as the occasional hypoxic conditions in the Kempenfelt Bay hypolimnion (Eimers et al., 2005). According to Dittrich et al. (2013), 58% of phosphorus release from the sediments occurs within a short time scale, while a substantial fraction (42%) of diagenetically mobile P in the sediments represents a long-term source in this site. The main basin received 48.5 tonnes P yr⁻¹ from the watershed and the adjacent basins, while 12.1 tonnes P yr⁻¹ were exported through the outflow (Atherley Narrows), resulting in a P retention (75%) that was quite close to the lake-wide estimate (83%). The sediments in the main basin are mostly driven by fast diagenetic processes of settling organic matter from lake epilimnion (Dittrich et al., 2013), which in turn may be partly reflected in our predictions of a 9.2 tonnes P yr⁻¹ internal P loading. Overall, consistent with Dittrich et al.'s (2013) estimates, our analysis suggests that the P diffusive fluxes from the sediments amount to less than 30–35% of the exogenous P loading in Lake Simcoe.

In a recent study, Nurnberg et al. (2013) attempted to quantify the long-term internal P loading in Lake Simcoe using two different methods: (i) an in situ estimation based on the difference of the TP concentrations between July and October; and (ii) a gross estimation based on the product of experimental P release rates with the

spatiotemporal hypoxic extent of the sediments (Loh et al., 2013). The whole lake internal P loading was estimated to be 37.4 tonnes P yr⁻¹ (53% of the external loading) and 62.9 tonnes P yr⁻¹ (89% of the external loading), respectively. Because of the significant discrepancy between our internal P fluxes and those reported by Nurnberg et al. (2013), we attempted to shed light on the implications for the predicted P cycling in Lake Simcoe. In particular, we simulated conditions of elevated internal P fluxes mediated through the sediments by assigning a higher fraction of egested/refiltered seston and metabolic excreta to be directly deposited onto the sediments in conjunction with increased sediment P mobility (Table 7). Consequently, the active dreissenid biodeposition increased from 22.4 to 111.3 tonnes P yr⁻¹ in eastern Lake Simcoe, from 9.7 to 49.5 tonnes P yr⁻¹ in main basin, and from 6.7 to 33.1 tonnes P yr⁻¹ in Cook's Bay, accompanied by an increase in the upward fluxes in the sediment–water column interface (difference between P release from sediments and particle settling) from –5.8 to –0.9, –32.3 to +0.6 and –3.9 to –2.9 tonnes P yr⁻¹, respectively. Notably, the ambient TP levels after the reallocation of the dreissenid egesta on the sediments could not be completely counterbalanced by (realistically) elevated sediment reflux rates, while any other calibration strategy invoking additional subsidies in the water column (e.g., intensification of macrophyte metabolic P release) resulted in a severe depletion of the sediment P pool. In this regard, we note that the unaccounted role of benthic algae could conceivably provide an alternative pathway of P recycling (Buzzelli et al., 2000), especially since measurements of the P tissue content in Lake Simcoe periphyton (e.g., *Dichotomosiphon tuberosus*) are comparable to the storage values reported for macrophytes (6–8 tonnes P). In all basins of Lake Simcoe, organic P (NaOH-NRP) represents a substantial part of P released from the sediments (Dittrich et al., 2013). Prior to 1995, phytoplankton biomass predominantly contributed to the organic P fraction (Eimers et al., 2005), but the periphyton (or biofilm) supported by macrophytes likely contributes to the currently elevated NaOH-NRP fraction, which in turn can be an indicator of the microbial activity in the sediments (Jaschinski et al., 2011).

In conclusion, we examined the relative importance of the causal linkages between exogenous loading and internal nutrient recycling with the P dynamics in Lake Simcoe, Ontario, Canada. Our intent was to examine whether the spatial and temporal variability of P, and broader effects to the ecosystem, were driven by the internal mechanisms of dreissenid activity, macrophyte proliferation, and the interplay between water column and sediments (Fig. 5). Consistent with empirical evidence from the system, our model predicts that macrophyte intake was responsible for a significant loss of P from the interstitial waters, thereby providing a significant pathway for the rapid transport of the nutrients assimilated from the sediments into the water column. Dreissenids filter a significant amount of particulate P from the water column, but the effective clearance rate is significantly lower with a substantial amount of the filtered particles (>85%) returned into the water column as faeces, pseudofeces or other metabolic excreta. This pattern is particularly pronounced in the shallow eastern end of Lake Simcoe, where a large portion is located within the euphotic and well-mixed zone, and therefore the elevated benthic photosynthesis and access of the dreissenids to sestonic algae create favourable conditions for biodeposition and nutrient recycling. Importantly, the large fetch

Table 7

TP fluxes (tonnes P yr⁻¹) from different mechanisms considered by the model under a characterization of faster sediment P release.

Site	water-sed	water-mac	water-ZM	sed-ZM	sed-Mac	Burial	Water in	Water out
Kbe	–0.3	1.7	–3.0	3.0	–1.7	0.7	9.3	7.0
KBh	–0.6	0.0	0.0	0.0	0.0	0.8	0.0	0.0
CBe	–2.1	34.0	–35.5	33.1	–33.8	0.9	18.3	13.8
CBh	–0.8	0.0	0.0	0.0	0.0	0.9	0.0	0.0
E1	–0.9	78.3	–108.4	111.3	–78.3	26.2	20.0	–8.1
MBe	–1.4	21.9	–19.3	20.0	–22.1	1.1	21.7	9.5
MBh	2.0	0.0	–27.9	29.5	0.0	33.0	0.0	0.0

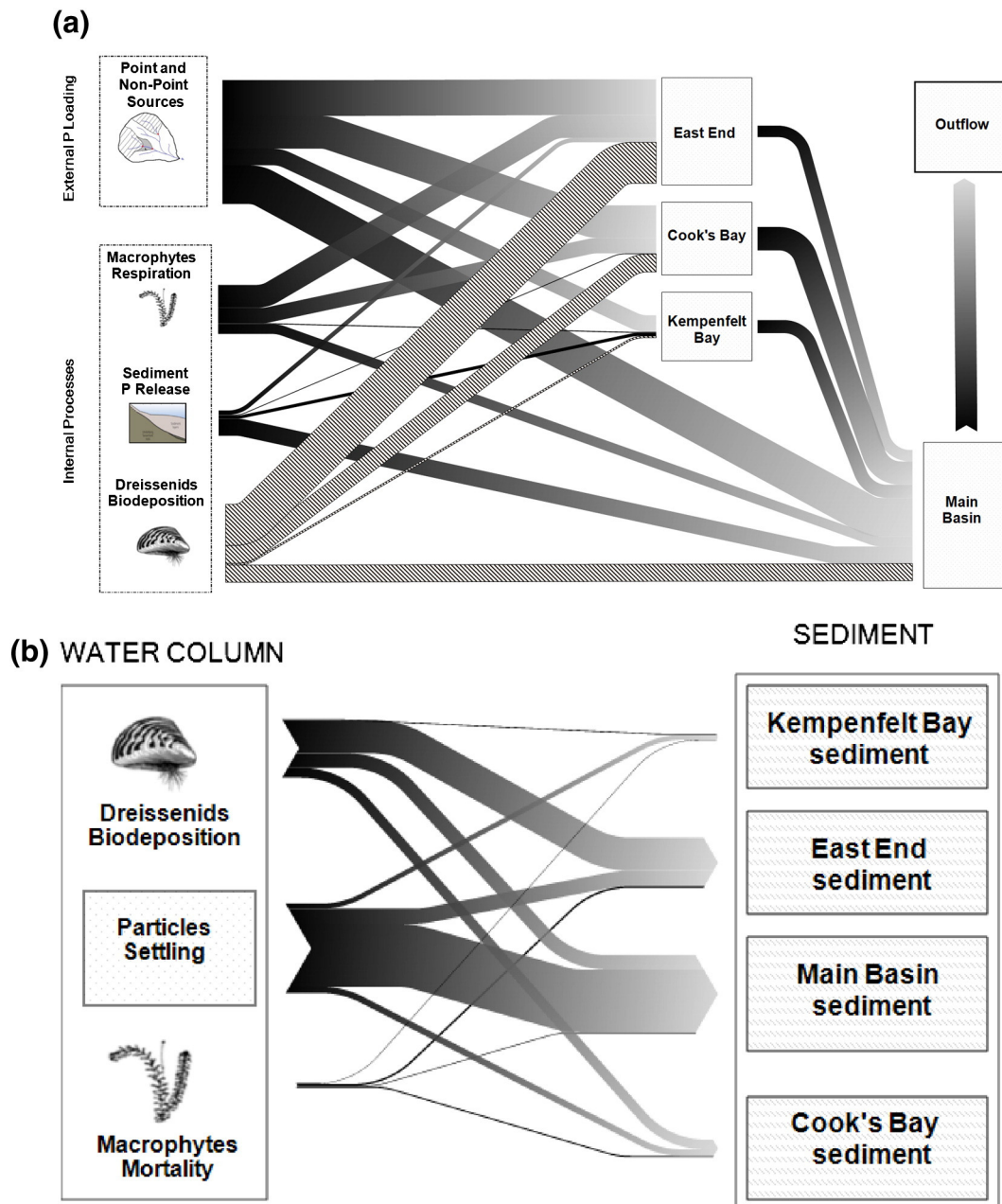


Fig. 5. (a) Sankey diagram for comparative description of the phosphorus flows from exogenous and endogenous P sources (tonnes P yr^{-1}). Width of the flow pathways is proportional to annual estimates of relevant fluxes. Dreissenids pathways indicate negative fluxes associated with the particle rejection/egestion of metabolic excreta minus particle filtration; (b) comparative diagram of P sinks at sediment–water interface (tonnes P yr^{-1}).

of Lake Simcoe and the fairly rapid hydrodynamic mixing may facilitate the localized impacts of dreissenids to modulate ecosystem-scale patterns. P diffusive fluxes from the sediments account for about 30–35% of the exogenous P loading in Lake Simcoe. The retention capacity in Cook's Bay is estimated to be about 28%, which is distinctly lower than estimates from the 1980s. Thus, the colonization of the embayment by dreissenids and the recent proliferation of macrophytes appear to have decreased the P retention in Cook's Bay, where the predominant fraction of TP is carbonate-bound P (apatite-P) mainly due to the accelerated erosion in the catchment. The sediments in the main basin are mostly driven by fast diagenetic processes of settling organic matter from the epilimnion, resulting in internal P loading of $9.2 \text{ tonnes P yr}^{-1}$. In a similar manner, the hypolimnetic sediments in Kempenfelt Bay

are responsible for a fairly high diffusive P flux into the water column ($\approx 1.7 \text{ tonnes P yr}^{-1}$), presumably reflecting the highest proportion of the redox-sensitive P sediment pool compared to other lake segments. Finally, regarding the absence of a decreasing trend in the lake P concentrations after the invasion of dreissenid mussels, we argue that the presence of active nutrient recycling pathways, potentially enhanced by the particular morphological features and water mass circulation patterns in Lake Simcoe, could offset the direct dreissenid filtration effects. We believe that the role of the different feedback loops associated with nutrient recycling should be explicitly considered from the on-going restoration efforts in Lake Simcoe, as it can considerably shape the relationship between external loading and ecosystem response in both space and time.

Acknowledgements

This project was undertaken with the financial support of the Government of Canada provided through the Department of the

Environment. Alexey Gudimov has also received financial support from a Doctoral Scholarship from the Natural Sciences and Engineering Research Council of Canada (CGSD2, 2012–2014). All the material pertinent to this analysis is available upon request from the corresponding author.

Appendix A. State variables and parameters of the total phosphorus model

Symbol	Variables and Parameters	Value	Unit
A_1	Sediment area:		m^2
A_1	Kempenfelt Bay epilimnion	5,795,000	
A_2	Kempenfelt Bay hypolimnion	29,942,500	
A_3	Cook's Bay epilimnion	26,220,000	
A_4	Cook's Bay hypolimnion	12,500,000	
A_5	East End epilimnion	124,630,000	
A_6	Main Basin epilimnion	46,445,000	
A_7	Main Basin hypolimnion	470,472,500	
A_{Lh}	Epilimnion/Hypolimnion interface		m^2
b_c	Exponent for weight effect on dreissenid ingestion	-0.39 ^a	
B_{mac}	Macrophyte biomass (dry weight)		$g\ m^{-2}$
B_{mac}^{total}	Total macrophyte biomass in a segment (dry weight)		MT
BP_{mac}	Phosphorus content in macrophyte biomass	0.0021 ^b	$g\ P\ g\ dry\ weight^{-1}$
BP_{zm}	Phosphorus content in dreissenid biomass	0.006 ^c	$g\ P\ g\ wet\ weight^{-1}$
b_r	Exponent for weight effect on respiration	-0.25 ^a	
b_{sdr}	Sediment bed shear stress exponent	1 ^d	
B_{sed-PP}	Burial rate of particulate phosphorus:		day^{-1}
B_{zm}	Dreissenid biomass		$g\ mussel\ WW\ ind^{-1}$
B_{zm}^{total}	Total lake dreissenid biomass		MT
chl_a	Chlorophyll α concentration		$\mu g\ L^{-1}$
chl_aC	Chlorophyll α to carbon ration in phytoplankton		0.05
DIP_{sed}	DIP in the sediments		$\mu g\ L^{-1}$
D_{crit}	Depth of frictional resistance		m
DIP_{sede}	Equilibrium phosphorus concentration in the solid phase of sediments		$\mu g\ L^{-1}$
DIP_w	DIP in the water column		$\mu g\ L^{-1}$
D_{mac}	Macrophyte mortality rate	0.001	day^{-1}
DO	Dissolved oxygen concentration		$mg\ O_2\ L^{-1}$
D_{sed}	Diffusion exchange rate between sediment pore water and water column		day^{-1}
D_{zm}	Dreissenid egestion and excretion		$g\ food\ g\ mussel^{-1}\ day^{-1}$
E	Langmuir sorption constant	9.5	$L\ mg^{-1}$
F	Wind fetch		m
FD	Time fraction of daily solar radiation		
$f_i(t)$	Temperature dependence of ingestion		
f_{OP-ZM}	Fraction of organic phosphorus in dreissenid excretion	0.6	
FR	Dreissenid filtration rate		$L\ g\ mussel^{-1}\ day^{-1}$
$f_r(t)$	Temperature dependence of respiration		
f_{resus}	Inorganic fraction of resuspended phosphorus	0.5	
FT_{zm}	Phosphorus mass filtered by dreissenids		$kg\ day^{-1}$
F_{zm}	Dreissenid egestion		$g\ food\ g\ mussel^{-1}\ day^{-1}$
G_{mac}	Macrophyte growth rate		day^{-1}
I_0	Solar radiation on the surface		$MJ\ m^{-2}\ day^{-1}$
H_s	Wave height		
I_{opt}	Optimal solar radiation for macrophyte growth	18	$MJ\ m^{-2}\ day^{-1}$
I_{zm}	Dreissenid food ingestion		$g\ food\ g\ mussel^{-1}\ day^{-1}$
k	Exponential decay coefficient in drift current equation		
K_1	Empirical coefficient representing temperature effect on ingestion at t_1	0.1 ^a	
K_2	Empirical coefficient representing temperature effect on ingestion at t_2	0.98 ^a	
K_3	Empirical coefficient representing temperature effect on ingestion at t_3	0.98 ^a	
K_4	Empirical coefficient representing temperature effect on ingestion at t_4	0.02 ^a	
K_{ad}	First-order desorption/sorption rate	7.2	day^{-1}
K_{cp}	Saturation particulate phosphorus concentration	1	$mg\ P\ L^{-1}$
K_{d20}	Decomposition rate coefficients at 20 °C		day^{-1}
	Kempenfelt Bay epilimnion	0.0025	
	Kempenfelt Bay hypolimnion	0.00075	
	Cook's Bay epilimnion	0.0078	
	Cook's Bay hypolimnion	0.0006	
	East End epilimnion	0.0006	
	Main Basin epilimnion	0.00065	
	Main Basin hypolimnion	0.00013	
K_{decom}	Sediment decomposition rate		day^{-1}
K_{diff}	Sediment diffusion exchange at reference temperature (20 °C)	7.38 10 ⁻¹⁰ ^e	$m^2\ day^{-1}$
K_{DO}	Half saturation constant for anaerobic phosphorus sediment release	0.5 ^d	$mg\ O_2\ L^{-1}$
K_{nstr}	Diffusivity in non-stratified conditions	10 (d)	$m^2\ day^{-1}$

(continued on next page)

Appendix A (continued)

Symbol	Variables and Parameters	Value	Unit
K_p	Half saturation constant for phosphate in sediment pore water	5	$\mu\text{g L}^{-1}$
K_{str}	Diffusivity in stratified conditions	0.15 ^d	$\text{m}^2 \text{day}^{-1}$
L_{seg}	Lake width between shores at cross section between adjacent segments		M
L_{zm}	Length of individual dreissenid		M
M_w	Flow per unit width due to orbital wave action		$\text{m}^2 \text{sec}^{-1}$
M_d	Flow per unit width in a drift current		$\text{m}^2 \text{sec}^{-1}$
N_{ab}	Abundance of zebra mussels per unit area	7,000 ^f	ind m^{-2}
OP_{sed}	Organic phosphorus in the sediments		mg g^{-1}
PC	Intracellular P:C ratio in phytoplankton	0.024	
PIP_{max}	Maximum sorption capacity		mg g^{-1}
	Kempenfelt Bay epilimnion	1	
	Kempenfelt Bay hypolimnion	1	
	Cook's Bay epilimnion	0.4	
	Cook's Bay hypolimnion	0.4	
	East End epilimnion	0.8	
	Main Basin epilimnion	0.8	
	Main Basin hypolimnion		
PIP_{sed}	PIP in the sediments		mg g^{-1}
P_m	Maximum gross photosynthesis rate	0.03	day^{-1}
PP_w	Particulate phosphorus in water		$\mu\text{g L}^{-1}$
P_{sdfzm}	Pseudofecal mass from dreissenids		kg day^{-1}
Q	Slope estimate, approximately Q10	3.1 ^a	
R_{mac}	Macrophyte respiration rate		day^{-1}
Q_{trib}	Tributary inflow from adjacent watershed		
$R_{\text{mac}20}$	Macrophyte respiration rate at 20°C	0.018 ^d	day^{-1}
R_{resus}	Sediment resuspension rate		kg day^{-1}
R_{zm}	Dreissenid respiration		$\text{g O}_2 \text{g mussel}^{-1} \text{day}^{-1}$
S_{bur}	Burial coefficient		m day^{-1}
	Kempenfelt Bay epilimnion	$5.86 \times 10^{-6\text{g}}$	
	Kempenfelt Bay hypolimnion	1.17×10^{-6}	
	Cook's Bay epilimnion	5.86×10^{-6}	
	Cook's Bay hypolimnion	5.86×10^{-6}	
	East End epilimnion	5.86×10^{-6}	
	Main Basin epilimnion	1.17×10^{-6}	
	Main Basin hypolimnion	2.34×10^{-6}	
SDA	Fraction of ingestion spent on feeding energy	0.285 ^a	
S_{sed}	Sediment desorption/sorption rate		day^{-1}
τ_s	Wind stress on water surface		N m^{-2}
T	Water temperature		°C
T_s	Wave period		sec
t_0	Optimum temperature for standard respiration	28 ^a	°C
t_1	Lower temperature at which consumption is K_1 x maximum ingestion	2 ^a	°C
t_2	Lower temperature at which consumption is K_2 x maximum ingestion	12 ^a	°C
t_3	Higher temperature at which consumption is K_3 x maximum ingestion	21 ^a	°C
t_4	Higher temperature at which consumption is K_4 x maximum ingestion	32 ^a	°C
t_m	Maximum temperature for standard respiration	31 ^a	°C
t_d	Minimum storm duration		minutes
$\text{TP}_{\text{backflow}}$	Total phosphorus fluxes through backflow transport from adjacent segment		$\mu\text{g L}^{-1} \text{day}^{-1}$
$\text{TP}_{\text{DLe,Lh}}$	Total phosphorus exchanges between epilimnion and hypolimnion		
TP_{in}	Total phosphorus fluxes from exogenous sources and antecedent segments		$\mu\text{g L}^{-1} \text{day}^{-1}$
TP_{macK}	Total phosphorus fluxes from macrophyte respiration		$\mu\text{g L}^{-1} \text{day}^{-1}$
TP_{out}	Total phosphorus outflow fluxes		$\mu\text{g L}^{-1} \text{day}^{-1}$
TP_{sdD}	Total phosphorus fluxes from sediment diffusion		$\mu\text{g L}^{-1} \text{day}^{-1}$
TP_{sdR}	Total phosphorus fluxes from resuspension		$\mu\text{g L}^{-1} \text{day}^{-1}$
TP_w	Total phosphorus concentration in the water column		$\mu\text{g L}^{-1}$
TP_{wS}	Total phosphorus settling		$\mu\text{g L}^{-1} \text{day}^{-1}$
TP_{zmF}	Total phosphorus filtration		$\mu\text{g L}^{-1} \text{day}^{-1}$
TP_{zmR}	Total phosphorus fluxes from dreissenid respiration		$\mu\text{g L}^{-1} \text{day}^{-1}$
TP_{zmRjw}	Total phosphorus fluxes from dreissenid rejection to water column		$\mu\text{g L}^{-1} \text{day}^{-1}$
TP_{zmX}	Total phosphorus fluxes from dreissenid excretion		$\mu\text{g L}^{-1} \text{day}^{-1}$
U_{zm}	Dreissenid excretion		$\text{g food g mussel}^{-1} \text{day}^{-1}$
U_a	Wind speed		m sec^{-1}
U_s	Surface current velocity		m sec^{-1}
V_w	Segment-specific volume as a function of time, determined by the water balance		m^3
V_s	Weighted average settling rate for phytoplankton and detritus particles		m day^{-1}
$V_{s\text{-chla}}$	Settling rate of phytoplankton	0.005	m day^{-1}
$V_{s\text{-pp}}$	Settling rate of organic matter other than phytoplankton	0.020	m day^{-1}
V_{sed}	Segment-specific sediment volume		m^3
w_{DIP}	Proportion of ambient dissolved phosphorus		
w_f	Conversion efficiency	1.724138 ^a	$\text{g mussel g food}^{-1}$
w_r	Respiration efficiency	5.586207 ^a	$\text{g mussel g O}_2^{-1}$
Z	Water depth		m
Z_{mac}	Water depth from the water surface to the top of macrophyte bed	4.3	m
α_1	Background extinction coefficient	0.24 ^h	m^{-1}

Appendix A (continued)

Symbol	Variables and Parameters	Value	Unit
α_2	Phytoplankton self shading effect	0.02	$\text{m}^2 \text{mg chl a}^{-1}$
α_c	Maximum dreissenid ingestion rate	1.86	$\text{mg food g mussel}^{-1} \text{day}^{-1}$
$\alpha_{c \text{ refit}}$	Maximum dreissenid ingestion rate scaled for water turbulence attenuation with depth to represent formation of concentration boundary layer at lake bed and enhanced refiltration		
α_f	Minimum fraction of food egested	0.315 ^a	
α_{mac}	Segment-specific fraction of macrophyte areal coverage		%
	Kempenfelt Bay epilimnion	25 ⁱ	
	Kempenfelt Bay hypolimnion	0	
	Cook's Bay epilimnion	68 ^h	
	Cook's Bay hypolimnion	0	
	East End epilimnion	20 ^h	
	Main Basin epilimnion	25 ^h	
	Main Basin hypolimnion	0	
α_{zm}	Segment-specific fraction of dreissenid areal colonization		%
	Kempenfelt Bay epilimnion	100 ^j	
	Kempenfelt Bay hypolimnion	0	
	Cook's Bay epilimnion	100	
	Cook's Bay hypolimnion	0	
	East End epilimnion	100	
	Main Basin epilimnion	100	
	Main Basin hypolimnion	53	
α_r	Maximum effective dreissenid respiration rate (including reproduction)	0.014	$\text{mg O}_2 \text{ g mussel}^{-1} \text{day}^{-1}$
α_{cr}	Clearance coefficient accounting for water turbulence attenuation with depth to represent enhanced refiltration and formation of concentration boundary layer at lake bed		
α_{sdr}	Resuspension coefficient	2	$\text{mg P m}^2 \text{day}^{-1}$
α_u	Fraction of assimilated food excreted	0.064 ^a	
α_{sed}	Fraction of filtered food biodeposited directly to sediment	0.01	
γ_f	Coefficient for egestion dependence on food availability	0.88 ^a	
δ	Sediment thickness		cm
	Kempenfelt Bay epilimnion	6.5 ^k	
	Kempenfelt Bay hypolimnion	2.0	
	Cook's Bay epilimnion	6.5	
	Cook's Bay hypolimnion	6.5	
	East End epilimnion	6.5	
	Main Basin epilimnion	6.5	
	Main Basin hypolimnion	6.0	
$\Delta \text{TP}_{\text{Le/Lh}}$	TP gradient between epilimnion and hypolimnion		$\mu\text{g L}^{-1}$
Δz	Distance between epilimnion and hypolimnion centroids		m
θ_d	Temperature coefficient for decomposition	1.08	
$\theta_{\text{r}_{\text{mac}}}$	Temperature dependence of macrophyte respiration	1.08	
θ_s	Temperature dependence of sediment diffusion	1.08	
ν_{sdr}	Sediment resuspension mass		$\text{kg m}^{-2} \text{day}^{-1}$
ρ	Sediment solid density	2.55 ⁱ	g cm^{-3}
ρ_a	Air density		Kg m^{-3}
τ_s	Wind stress on water surface		N m^{-2}
τ	Sediment bed shear stress		N m^{-2}
τ_c	Critical sediment bed shear stress	0.03 ^d	N m^{-2}
φ	Sediment porosity	0.947 ^h	
\varnothing	Latitude	44.39°N	grad

^a Schneider, 1992.^b Depew et al., 2011b^c Nalepa et al., 1991.^d Kim et al., 2013.^e Yuan-Hui and Gregory, 1974.^f Evans et al., 2011.^g Hiriart-Baer et al., 2011.^h Depew et al., 2011a, 2011b.ⁱ Ginn, 2011.^j Ozersky et al., 2011; Ozersky et al., 2013; Evans et al., 2011; Schwab et al., 2013.^k Dittrich et al., 2013.^l Avnimelech et al., 2001; McCulloch et al., 2013.

Appendix B. Supplementary data

Supplementary data to this article can be found online at <http://dx.doi.org/10.1016/j.ecoinf.2014.11.007>.

References

- Arhonditsis, G.B., Brett, M.T., 2005. Eutrophication model for Lake Washington (USA): Part II – model calibration and system dynamics analysis. *Ecol. Model.* 187, 179–200.
- Asaeda, T., Trung, V.K., Manatunge, J., 2000. Modelling the effects of macrophyte growth and decomposition on the nutrient budget in shallow lakes. *Aquat. Bot.* 68 (3), 217–237.
- Avnimelech, Y., Ritvo, G., Meijer, L.E., Kochba, M., 2001. Water content, organic carbon and dry bulk density in flooded sediments. *Aquacult. Eng.* 25, 25–33.

- Baird, Associates, 2006. Lake Simcoe Hydrodynamic and Water Quality Model.
- Barko, J.W., James, W.F., 1998. Effects of submerged aquatic macrophytes on nutrient dynamics, sedimentation, and resuspension. In: Jeppesen, E., Søndergaard, M., Christoffersen, K. (Eds.), *The Structuring Role of Submerged Macrophytes in Lakes*. Springer-Verlag, New York, pp. 197–214.
- Bierman, V.J., Kaur, J., DePinto, J.V., Feist, T.J., Dilks, D.W., 2005. Modelling the role of zebra mussels in the proliferation of blue-green algae in Saginaw Bay, Lake Huron. *J. Great Lakes Res.* 31 (1), 32–55.
- Bini, L., Thomaz, S., Carvalho, P., 2010. Limnological effects of *Egeria najas* Planchon (Hydrocharitaceae) in the arms of Itaipu Reservoir (Brazil, Paraguay). *Limnology* 11 (1), 39–47.
- Boegman, L., Loewen, M., Hamblin, P., Culver, D., 2008. Vertical mixing and weak stratification over zebra mussel colonies in western Lake Erie. *Limnol. Oceanogr.* 53 (3), 1093.
- Buzzelli, C.P., Childers, D.L., Dong, Q., Jones, R.D., 2000. Simulation of periphyton phosphorus dynamics in Everglades National Park. *Ecol. Model.* 134 (1), 103–115.
- Chao, X., Jia, Y., Shields Jr., F.D., Wang, S.S.Y., Cooper, C.M., 2008. Three-dimensional numerical modelling of cohesive sediment transport and wind wave impact in a shallow oxbow lake. *Adv. Water Resour.* 31 (7), 1004–1014.
- Chapra, S.C., Dolan, D.M., 2012. Great Lakes total phosphorus revisited: 2. Mass balance modelling. *J. Great Lakes Res.* 38 (4), 741–754.
- Christensen, K.K., 1999. Comparison of iron and phosphorus mobilization from sediments inhabited by *Littorella uniflora* and *Sphagnum* sp. at different sulfate concentrations. *Arch. Hydrobiol.* 145 (3), 257–275.
- Coastal Engineering Research Center (CERC), 1994. Shore Protection Manual. U.S. Army Corps of Eng, Washington, D.C.
- Coleman, F.C., Williams, S.L., 2002. Overexploiting marine ecosystem engineers: potential consequences for biodiversity. *Trends Ecol. Evol.* 17 (1), 40–44.
- Coughlan, J., 1969. The estimation of filtering rate from the clearance of suspensions. *Mar. Biol.* 2 (4), 356–358.
- Daunys, D., Zemlys, P., Olenin, S., Zaiko, A., Ferrarin, C., 2006. Impact of the zebra mussel *Dreissena polymorpha* invasion on the budget of suspended material in a shallow lagoon ecosystem. *Helgol. Mar. Res.* 60 (2), 113–120.
- Depew, D.C., Houben, A.J., Ozersky, T., Hecky, R.E., Guildford, S.J., 2011a. Why does “Cladophora” fail to reach nuisance proportions in Lake Simcoe? *J. Great Lakes Res.* 37, 90–102.
- Depew, D.C., Houben, A.J., Ozersky, T., Hecky, R.E., Guildford, S.J., 2011b. Submerged aquatic vegetation in Cook’s Bay, Lake Simcoe: assessment of changes in response to increased water transparency. *J. Great Lakes Res.* 37, 72–82.
- Dittrich, M., Chesnyuk, A., Gudimov, A., McCulloch, J., Quaizi, S., Young, J., Winter, J., Stainsby, E., Arhonditsis, G., 2013. Phosphorus retention in a mesotrophic lake under transient loading conditions: insights from a sediment phosphorus binding form study. *Water Res.* 47 (3), 1433–1447.
- Edwards, W.J., Rehmann, C.R., McDonald, E., Culver, D.A., 2005. The impact of a benthic filter feeder: limitations imposed by physical transport of algae to the benthos. *Can. J. Fish. Aquat. Sci.* 62 (1), 205–214.
- Eimers, M.C., Winter, J.G., Scheider, W.A., Watmough, S.A., Nicholls, K.H., 2005. Recent changes and patterns in the water chemistry of Lake Simcoe. *J. Great Lakes Res.* 31 (3), 322–332.
- Eriksson, P.G., Weisner, S.E.B., 1999. An experimental study on effects of submersed macrophytes on nitrification and denitrification in ammonium-rich aquatic systems. *Limnol. Oceanogr.* 44 (8), 1993–1999.
- Evans, D.O., 2007. Effects of hypoxia on scope-for-activity and power capacity of lake trout (*Salvelinus namaycush*). *Can. J. Fish. Aquat. Sci.* 64 (2), 345–361.
- Evans, D.O., Skinner, A.J., Allen, R., McMurtry, M.J., 2011. Invasion of zebra mussel, “*Dreissena polymorpha*”, in Lake Simcoe. *J. Great Lakes Res.* 37, 36–45.
- Ginn, B.K., 2011. Distribution and limnological drivers of submerged aquatic plant communities in Lake Simcoe (Ontario, Canada): utility of macrophytes as bioindicators of lake trophic status. *J. Great Lakes Res.* 37, 83–89.
- Gudimov, A., Ramin, M., Labencki, T., Wellen, C., Shelar, M., Shimoda, Y., Boyd, D., Arhonditsis, G.B., 2011. Predicting the response of Hamilton Harbour to the nutrient loading reductions: a modeling analysis of the “ecological unknowns”. *J. Great Lakes Res.* 37, 494–506.
- Gudimov, A., O’Connor, E., Dittrich, M., Jarjanazi, H., Palmer, M.E., Stainsby, E.A., Winter, J.G., Young, J.D., Arhonditsis, G.B., 2012. Continuous Bayesian network for studying the causal links between phosphorus loading and plankton patterns in Lake Simcoe, Ontario, Canada. *Environ. Sci. Technol.* 46 (13), 7283–7292.
- Hecky, R., Smith, R.E., Barton, D., Guildford, S., Taylor, W., Charlton, M., Howell, T., 2004. The nearshore phosphorus shunt: a consequence of ecosystem engineering by dreissenids in the Laurentian Great Lakes. *Can. J. Fish. Aquat. Sci.* 61 (7), 1285–1293.
- Higgins, S., Zanden, M.V., 2010. What a difference a species makes: a meta-analysis of dreissenid mussel impacts on freshwater ecosystems. *Ecol. Monogr.* 80 (2), 179–196.
- Hiriart-Baer, V.P., Milne, J.E., Marvin, C.H., 2011. Temporal trends in phosphorus and lacustrine productivity in Lake Simcoe inferred from lake sediment. *J. Great Lakes Res.* 37 (4), 764–771.
- Howard-Williams, C., Allanson, B.R., 1981. Phosphorus cycling in a dense *Potamogeton pectinatus* L. Bed. *Oecologia* 49 (1), 56–66.
- Jaschinski, S., Brepohl, D.C., Sommer, U., 2011. The trophic importance of epiphytic algae in a freshwater macrophyte system (*Potamogeton perfoliatus* L.): stable isotope and fatty acid analyses. *Aquat. Sci.* 73 (1), 91–101.
- Jimenez, A., Rennie, M.D., Sprules, W.G., La Rose, J., 2011. Temporal changes in the benthic invertebrate community of Lake Simcoe, 1983–2008. *J. Great Lakes Res.* 37, 103–112.
- Johnson, M.G., Nicholls, K.H., 1989. Temporal and spatial variability in sediment and phosphorus loads to Lake Simcoe, Ontario. *J. Great Lakes Res.* 15 (2), 265–282.
- Kim, D.-K., Zhang, W., Rao, Y.R., Watson, S., Mugalingam, S., Labencki, T., Dittrich, M., Morley, A., Arhonditsis, G.B., 2013. Improving the representation of internal nutrient recycling with phosphorus mass balance models: a case study in the Bay of Quinte, Ontario, Canada. *Ecol. Model.* 256, 53–68.
- Lick, W., 1986. Modelling the transport of fine-grained sediments in aquatic systems. *Sci. Total Environ.* 55, 219–228.
- Loh, P.S., Molot, L.A., Nurnberg, G.K., Watson, S.B., Ginn, B., 2013. Evaluating relationships between sediment chemistry and anoxic phosphorus and iron release across three different water bodies. *Inland Waters* 3 (1), 105–118.
- LSRCA, 2011. Aquatic plants in Lake Simcoe: distribution, environmental controls and utility as ecological indicators. *Lake Simcoe Region Conservation Authority*. Technical Progress Series in Lake Monitoring: Report No. 1.
- LSRCA, MOE, 2006. Annual Water Balances, Total Phosphorus Budgets and Total Nitrogen and Chloride Loads to Lake Simcoe (1998–2004). *Lake Simcoe Region Conservation Authority*.
- LSRCA, MOE, 2012. Annual Water Balances, Total Phosphorus Budgets and Total Nitrogen and Chloride Loads to Lake Simcoe (2004–2007). *Lake Simcoe Region Conservation Authority*.
- Maccoux, M.J., Dolan, D.M., Chapra, S.C., 2013. Chloride and total phosphorus budgets for Green Bay, Lake Michigan. *J. Great Lakes Res.* 39, 420–428.
- McCulloch, J., Gudimov, A., Arhonditsis, G., Chesnyuk, A., Dittrich, M., 2013. Dynamics of P-binding forms in sediments of a mesotrophic hard-water lake: insights from non-steady state reactive-transport modelling, sensitivity and identifiability analysis. *Chem. Geol.* 354, 216–232.
- Mehta, A.J., Parchure, T.M., Dixit, J.G., Ariathurai, R., 1982. Resuspension potential of deposited cohesive sediment beds. In: Kennedy, V.S. (Ed.), *Estuarine Comparisons*. Academic Press, New York, pp. 591–609.
- Mian, M.H., Yanful, E.K., 2004. Analysis of wind-driven resuspension of metal mine sludge in a tailings pond. *J. Environ. Eng. Sci.* 3 (2), 119–135.
- Nalepa, T., Gardner, W., Malczyk, J., 1991. Phosphorus cycling by mussels (Unionidae: Bivalvia) in Lake St. Clair. *Environmental Assessment and Habitat Evaluation of the Upper Great Lakes Connecting Channels*. Springer, pp. 239–250.
- Nicholls, K.H., 1997. A limnological basis for a Lake Simcoe phosphorus loading objective. *Lake Res. Manag.* 13 (3), 189–198.
- Nicholls, K.H., Heintsch, L., Carney, E., 2002. Univariate step-trend and multivariate assessments of the apparent effects of P loading reductions and zebra mussels on the phytoplankton of the Bay of Quinte, Lake Ontario. *J. Great Lakes Res.* 28 (1), 15–31.
- North, R.L., 2013. The state of Lake Simcoe (Ontario, Canada), the effects of multiple stressors on phosphorus and oxygen dynamics. *Inland Waters* 3 (1), 51–74.
- Nürnberg, G.K., LaZerte, B.D., Loh, P.S., Molot, L.A., 2013. Quantification of internal phosphorus load in large, partially polymictic and mesotrophic Lake Simcoe, Ontario. *J. Great Lakes Res.* 39 (2), 271–279.
- Omlin, M., Brun, P., Reichert, P., 2001. Biogeochemical model of Lake Zürich: sensitivity, identifiability and uncertainty analysis. *Ecol. Model.* 141, 105–123.
- Ozersky, T., Barton, D.R., Depew, D.C., Hecky, R.E., Guildford, S.J., 2011. Effects of water movement on the distribution of invasive dreissenid mussels in Lake Simcoe, Ontario. *J. Great Lakes Res.* 37, 46–54.
- Ozersky, T., Barton, D.R., Hecky, R.E., Guildford, S.J., 2013. Dreissenid mussels enhance nutrient efflux, periphyton quantity and production in the shallow littoral zone of a large lake. *Biol. Invasions* 15 (12), 2799–2810.
- Ramin, M., Stremilov, S., Labencki, T., Gudimov, A., Boyd, D., Arhonditsis, G.B., 2011. Integration of numerical modelling and Bayesian analysis for setting water quality criteria in Hamilton Harbour, Ontario, Canada. *Environ. Model. Softw.* 26 (4), 337–353.
- Rennie, M.D., Evans, D.O., 2012. Decadal changes in benthic invertebrate biomass and community structure in Lake Simcoe. *Freshw. Sci.* 31 (3), 733–749.
- Rørslett, B., Berge, D., Johansen, S.W., 1986. Lake enrichment by submersed macrophytes: a Norwegian whole-lake experience with *Elodea canadensis*. *Aquat. Bot.* 26, 325–340.
- Sand-Jensen, K., 1998. Influence of submerged macrophytes on sediment composition and near-bed flow in lowland streams. *Freshw. Biol.* 39 (4), 663–679.
- Schneider, D.W., 1992. A bioenergetics model of zebra mussel, *Dreissena polymorpha*, growth in the Great Lakes. *Can. J. Fish. Aquat. Sci.* 49 (7), 1406–1416.
- Schwalb, A., Bouffard, D., Ozersky, T., Boegman, L., Smith, R.E.H., 2013. Impacts of hydrodynamics and benthic communities on phytoplankton distributions in a large, dreissenid-colonized lake (Lake Simcoe, Ontario, Canada). *Inland Waters* 3 (2), 269–284.
- Smith, I., 1979. Hydraulic conditions in isothermal lakes. *Freshw. Biol.* 9 (2), 119–145.
- Sprung, M., Rose, U., 1988. Influence of food size and food quantity on the feeding of the mussel *Dreissena polymorpha*. *Oecologia* 77 (4), 526–532.
- Stantec, 2007. Aquatic macrophyte survey of Cook’s Bay, Lake Simcoe, August 2006. Report for LSRCA.
- Stow, C.A., Roessler, C., Borsuk, M.E., Bowen, J.D., Reckhow, K.H., 2003. Comparison of estuarine water quality models for total maximum daily load development in Neuse River Estuary. *J. Water Res. Pl.-ASCE* 129 (4), 307–314.
- Tsai, C.-H., Lick, W., 1986. A portable device for measuring sediment resuspension. *J. Great Lakes Res.* 12 (4), 314–321.
- Tsanis, I.K., 1992. Hydrodynamic computer model of major water movement patterns in lake simcoe. *Hydroflux Engineering Technical Report: Imp. B.14*.
- Vanderploeg, H.A., Liebig, J.R., Carmichael, W.W., Agy, M.A., Johengen, T.H., Fahnenstiel, G.L., Nalepa, T.F., 2001. Zebra mussel (*Dreissena polymorpha*) selective filtration promoted toxic Microcystis blooms in Saginaw Bay (Lake Huron) and Lake Erie. *Can. J. Fish. Aquat. Sci.* 58 (6), 1208–1221.
- Walz, N., 1978. The energy balance of the freshwater mussel *Dreissena polymorpha* Pallas in laboratory experiments and in Lake Constance. I. Pattern of activity, feeding and assimilation efficiency. *Arch. Hydrobiol. Suppl.* 55 (1), 83–105.

- Wang, H., Appan, A., Gulliver, J.S., 2003a. Modelling of phosphorus dynamics in aquatic sediments: I—model development. *Water Res.* 37 (16), 3928–3938.
- Wang, H., Appan, A., Gulliver, J.S., 2003b. Modelling of phosphorus dynamics in aquatic sediments: II—examination of model performance. *Water Res.* 37 (16), 3939–3953.
- Wigand, C., Stevenson, J.C., Cornwell, J.C., 1997. Effects of different submersed macrophytes on sediment biogeochemistry. *Aquat. Bot.* 56 (3–4), 233–244.
- Young, J.D., Winter, J.G., Molot, L., 2011. A re-evaluation of the empirical relationships connecting dissolved oxygen and phosphorus loading after dreissenid mussel invasion in Lake Simcoe. *J. Great Lakes Res.* 37, 7–14.
- Yu, N., Culver, D.A., 1999. Estimating the effective clearance rate and refiltration by zebra mussels, *Dreissena polymorpha*, in a stratified reservoir. *Freshw. Biol.* 41 (3), 481–492.
- Yuan-Hui, L., Gregory, S., 1974. Diffusion of ions in sea water and in deep-sea sediments. *Geochim. Cosmochim. Acta* 38, 703–714.
- Zhang, W., Kim, D.-K., Rao, Y.R., Watson, S., Mugalingam, S., Labencki, T., Dittrich, M., Morley, A., Arhonditsis, G.B., 2013. Can simple phosphorus mass balance models guide management decisions? A case study in the Bay of Quinte, Ontario, Canada. *Ecol. Model.* 257, 66–79.
- Zimmer, K.D., Hanson, M.A., Buttler, M.G., 2001. Influences of fathead minnows and aquatic macrophytes on nutrient partitioning and ecosystem structure in two prairie wetlands. *Arch. Hydrobiol.* 150 (3), 411–433.

**EXAMINATION OF THE ROLE OF DREISSENIDS AND MACROPHYTES IN
THE PHOSPHORUS DYNAMICS OF LAKE SIMCOE, ONTARIO, CANADA**

[ELECTRONIC SUPPLEMENTARY MATERIAL]

**Alexey Gudimov¹, Dong-Kyun Kim¹, Michelle E. Palmer², Joelle D. Young²,
Maria Dittrich¹, Jennifer G. Winter², Eleanor Stainsby², George B. Arhonditsis^{1*}**

¹Department of Physical & Environmental Sciences, University of Toronto,
Toronto, Ontario, Canada, M1C 1A4

²Great Lakes Water Monitoring & Reporting Section, Ontario Ministry of the Environment,
Environmental Monitoring and Reporting Branch, Toronto, Ontario, Canada, M9P 3V6

* Corresponding author

e-mail: georgea@utsc.utoronto.ca, Tel.: +1 416 208 4858; Fax: +1 416 287 7279.

Figures

Figure 1: Sensitivity of *TP* predictions on macrophyte light limitation: *black lines*: reference simulation; gray lines represent scenarios: a) *dotted line*: scenario of light deficiency ($\alpha_1=0.3$, $\alpha_2=0.025$), b) *dash-dot line*: scenario of optimal illumination of the water column ($\alpha_1=0.18$, $\alpha_2=0.015$); *gray solid line*: scenario of increased water clarity coupled with an increase of the optimal solar radiation for macrophyte growth ($\alpha_1=0.18$, $\alpha_2=0.015$, $I_{opt}=34$).

Figure 2: Sensitivity of *TP* predictions on macrophyte phosphorus limitation: *black lines*: reference simulation; *dotted line*: high affinity for phosphorus ($K_p=3.8$); *dash dot line*: low affinity for phosphorus ($K_p=6.3$).

Figure 3: Sensitivity of *TP* predictions on phosphorus recycling regimes mediated by macrophytes: *black lines*: reference simulation; *dotted line*: fast macrophytes growth and metabolic rates and fast sediment decomposition rates ($P_m=0.03+50\%$, $R_{mac20}=0.018+50\%$, $D_{mac}=0.001+15\%$, $K_{d20}=+50\%$ increase to the segment-specific value); *dash-dot line*: fast macrophytes growth and metabolic rates and slow sediment decomposition rates ($P_m=0.03+50\%$, $R_{mac20}=0.018+50\%$, $D_{mac}=0.001+15\%$, $K_{d20}=-50\%$ increase to the segment-specific value); *gray solid line*: slow macrophytes growth and metabolic rates and slow sediment decomposition rates ($P_m=0.03-50\%$, $R_{mac20}=0.018-50\%$, $D_{mac}=0.001-15\%$, $K_{d20}=-50\%$ increase to the segment-specific value).

Figure 4: Projected biomass response of submerge aquatic macrophytes in Cook's Bay according to scenarios of Holland Marsh P loading from 1999-2007 (18.3 metric tonnes or MT

P/year), 1990-1993 (56.0 MT P/year), and 1999-2007 loading coupled with legacy P in older sediments (22 cm).

Figure 5: Sensitivity of TP predictions on different dreissenids colonization densities: *black lines*: reference simulation; *gray dotted line*: areal abundance of 1000 ind/m²; *gray dot-dash line*: areal abundance of 10,000 ind/m².

Figure 6: Sensitivity of TP predictions on phosphorus recycling regimes mediated by dreissenids: *black lines*: reference simulation; *gray dotted line*: fast dreissenid ingestion and respiration rates and fast sediment decomposition rates ($a_c, a_r, K_{d20} = \text{reference} + 25\%$); *gray dash-dot line*: slow dreissenid ingestion and respiration rates and slow sediment decomposition rates ($a_c, a_r, K_{d20} = \text{reference} - 25\%$).

Figure 7: Sensitivity of TP predictions on sediment porosity: *black lines*: reference simulation; *gray dotted line*: high sediment porosity ($\phi=0.98$); *gray dash-dot line*: low sediment porosity ($\phi=0.85$))

Figures 8: Sensitivity of TP predictions on phosphorus adsorption/desorption processes in the sediments: *black lines*: reference simulation; *gray dotted line*: predominance of adsorption fluxes ($K_{ad}=5.4, PIP_{max}=1, E=10.925$), *gray dash-dotted line*: predominance of desorption fluxes ($K_{ad}=7.56, PIP_{max}=0.6, E=9.025$).

Figure 9: Sensitivity of *TP* predictions on phosphorus diffusion from the sediments: *black lines*: reference simulation; *gray dotted line*: high diffusivity with thicker sediments (K_{diff} , $\delta=125\%$); *gray dash-dotted line*: low diffusivity with thinner sediments (K_{diff} , $\delta=75\%$).

Figure 1

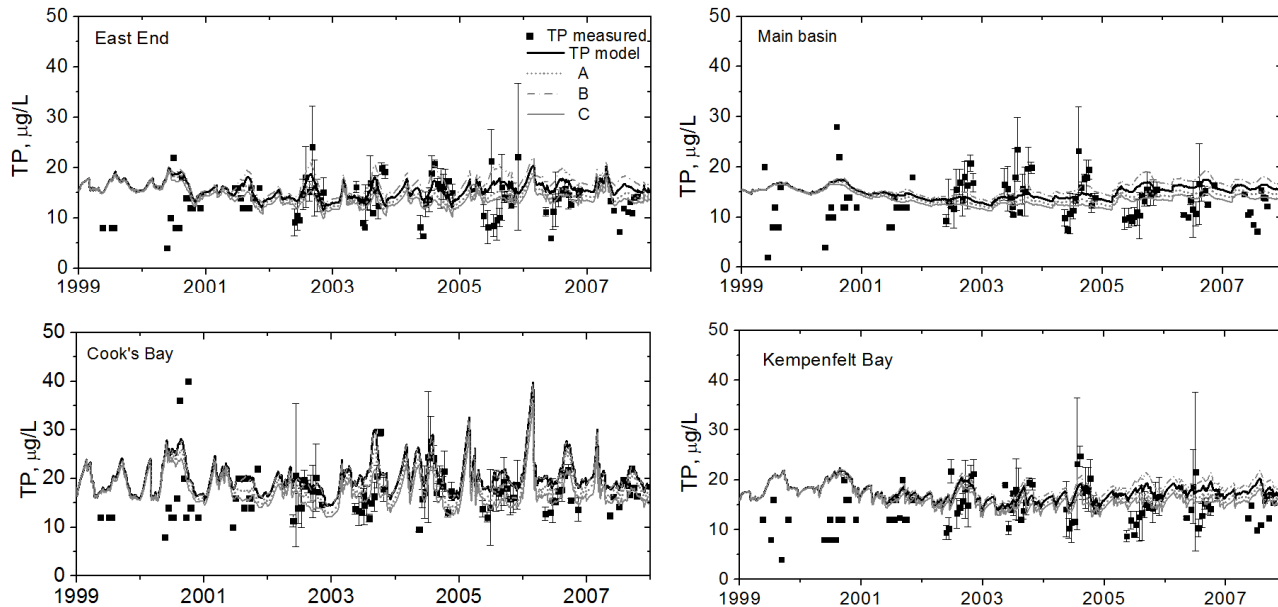


Figure 2

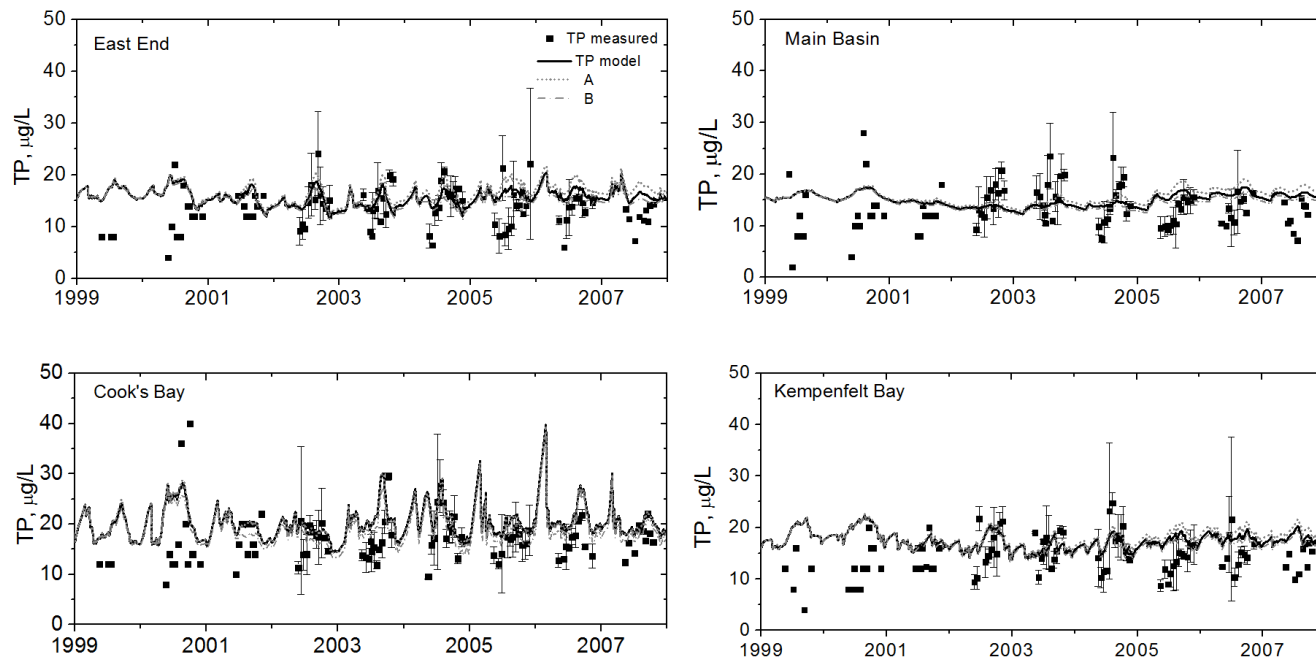


Figure 3

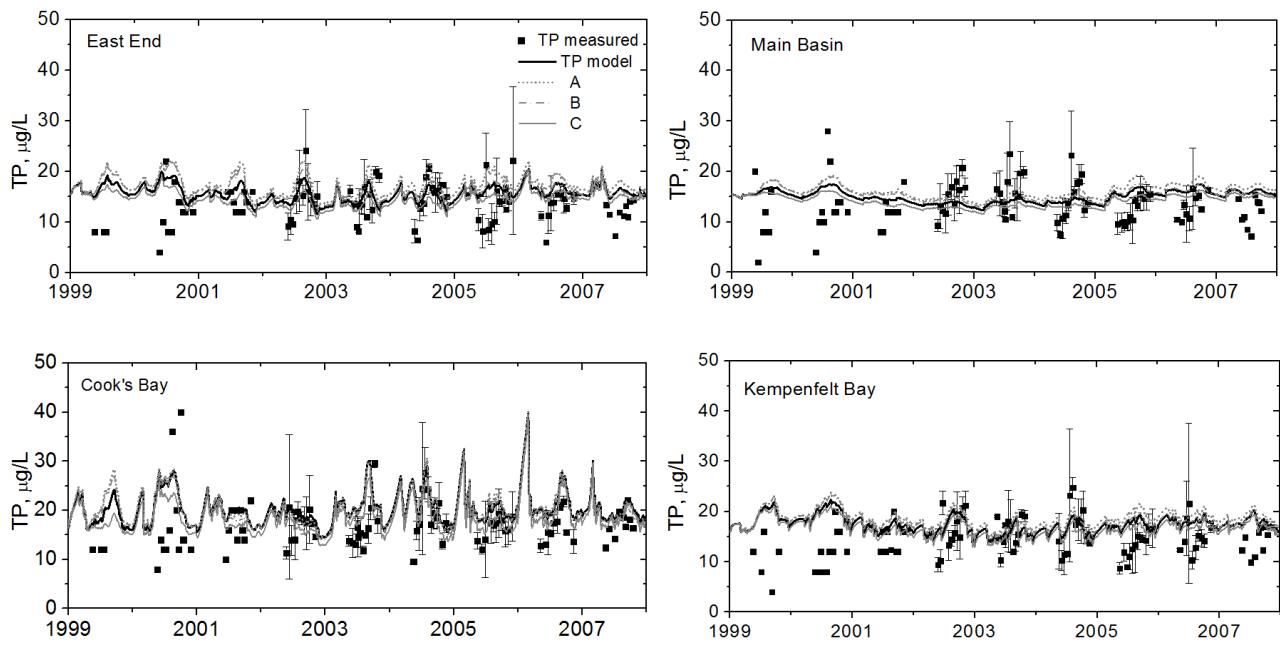


Figure 4

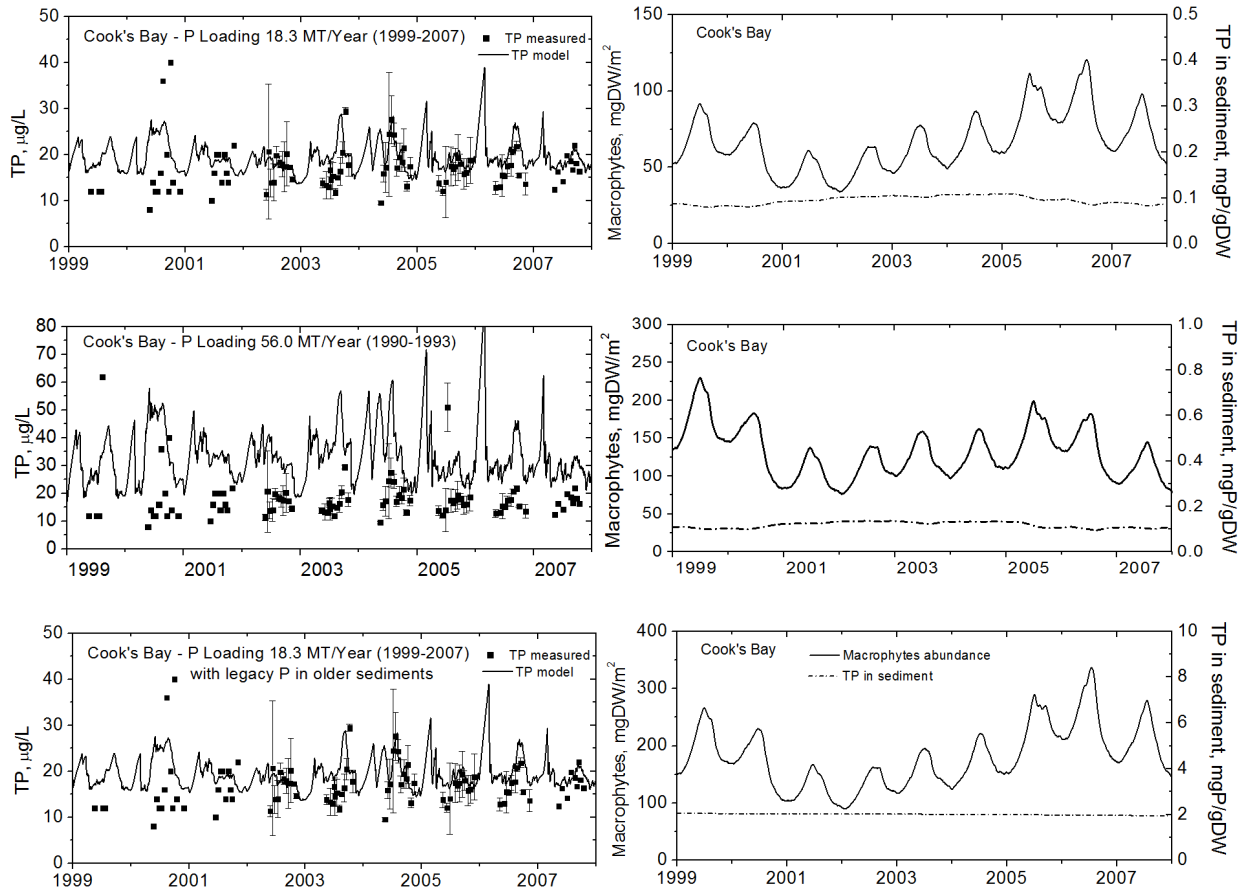


Figure 5

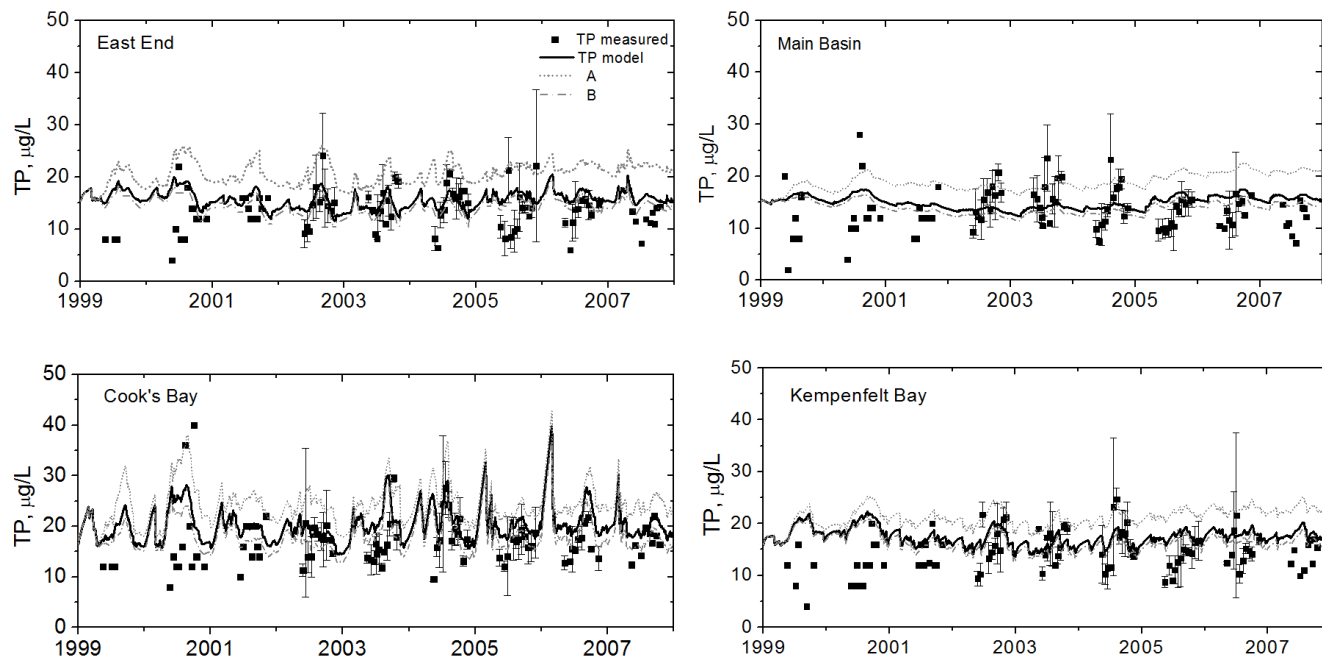


Figure 6

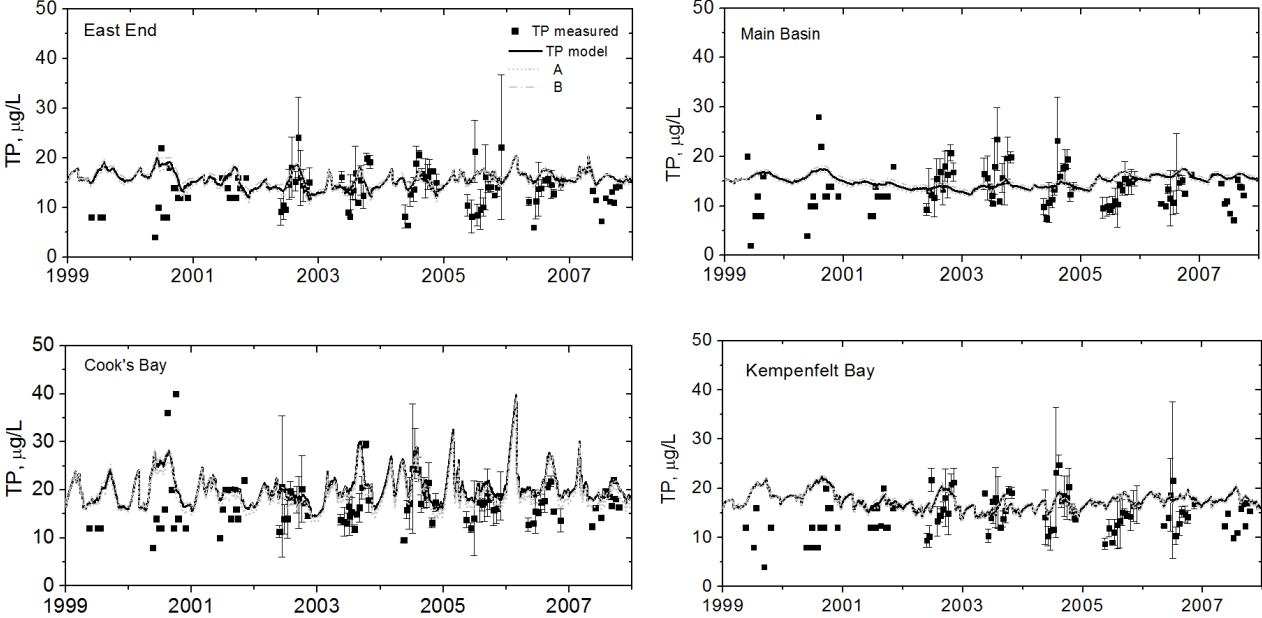


Figure 7

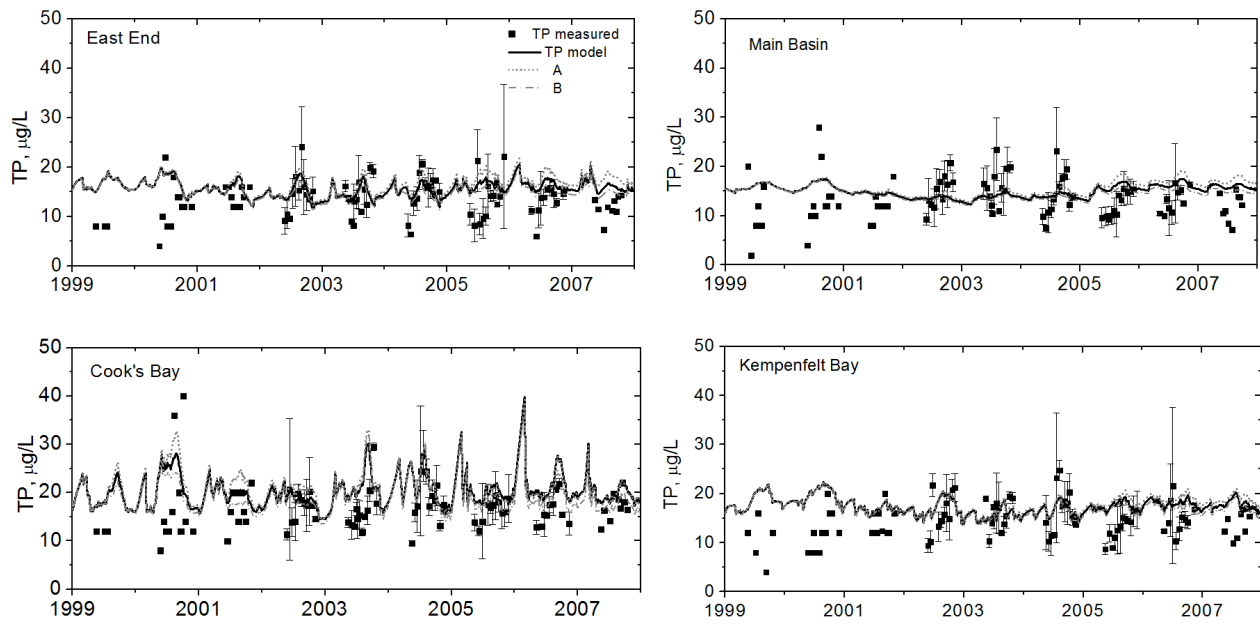


Figure 8

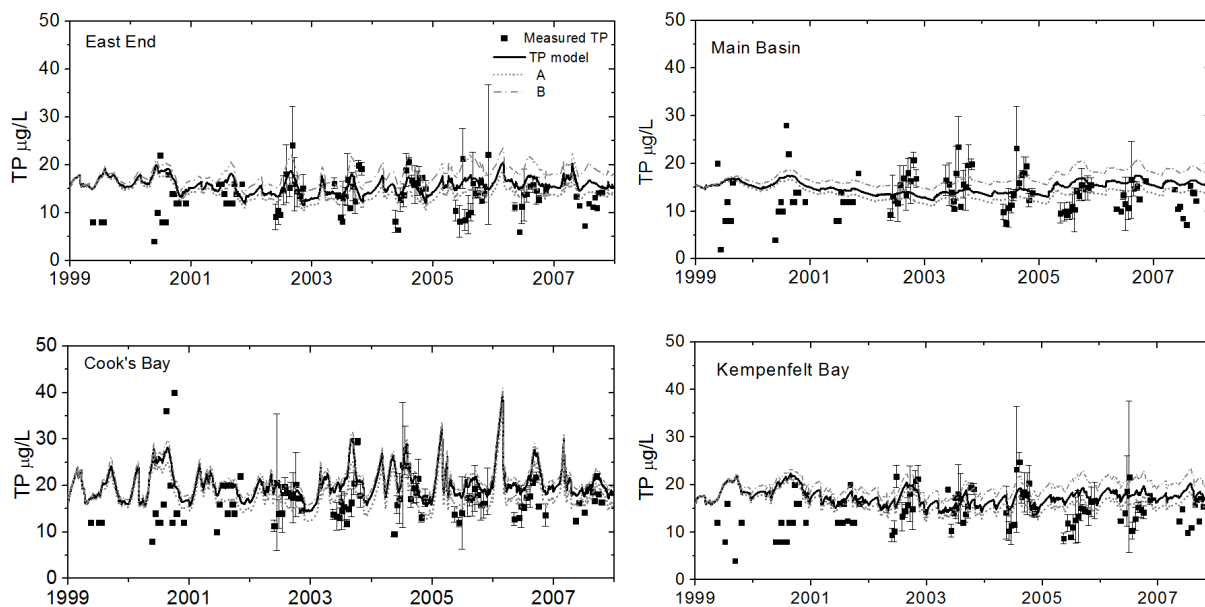


Figure 9

